1-1-2011

Cardiac Calsequestrin Phosphorylation And Trafficking In The Mammalian Cardiomyocyte

Timothy Mcfarland
Wayne State University

CARDIAC CALSEQUESTRIN PHOSPHORYLATION AND TRAFFICKING IN THE MAMMALIAN CARDIOMYOCYTE

by

TIMOTHY P. MCFARLAND

DISSERTATION

Submitted to the Graduate School

of Wayne State University,

Detroit, Michigan

in partial fulfillment of the requirements

for the degree of

DOCTOR OF PHILOSOPHY

2011

MAJOR: PHYSIOLOGY

Approved by:

_____

Advisor Date

_____

_____

_____

_____

DEDICATION

This work is dedicated to my family. To my parents and grandparents, who provided continuous support and footed the bill for the past ten years, thank you. Your investment finally paid off. And to my beautiful and patient wife Lindsay, thank you for getting me through the tough times and keeping our family afloat, I love you.

ACKNOWLEDGEMENTS

I would like to thank the members of my dissertation committee for their support and forwardness throughout this process. Your honesty and exceptional insights have helped me to develop professionally and have greatly expedited my graduation. I would especially like to thank my mentor Dr. Steven Cala for helping me to become a scientist. It's amazing that you were able to give me the time that you did.

TABLE OF CONTENTS

LIST OF TABLES

LIST OF FIGURES

CHAPTER 1

GENERAL INTRODUCTION

BACKGROUND AND SIGNIFICANCE

Cardiac biology

The cardiovascular system is responsible for transporting the many constituents of blood including electrolytes, nutrients, gases, and hormones, to and from all organs in the body. Without the heart to create the appropriate amount of positive pressure, organ perfusion would not occur, pH would become out of balance, and cellular homeostasis would become severely disrupted. The general physiology and anatomy of the heart are well defined (Fig. 1A,B). During the cardiac cycle, deoxygenated blood enters the right atrium through either the superior or inferior vena cava and is then pumped through the tricuspid valve into the right ventricle. It is then pushed through the pulmonic valve into the pulmonary arteries and pulmonary circulation where it is reoxygenated in the lungs. The oxygenated blood re-enters the heart at the left atrium by means of the pulmonary veins. Ventricular diastole then ensues, during which ventricular muscle relaxes. Pressure decreases in the left ventricle, and blood begins to enter through the mitral valve which is forced shut after a critical volume is reached. Contraction of the left atrium pushes a small amount of blood into the nearly full ventricle, increasing its pressure just prior to ventricular systole. Immediately after, left ventricular muscle cells contract and force the oxygenated blood through the aortic valve into the aorta and subsequent arterial circulation [1].

The left ventricular wall of the heart is responsible for generating the immense pressure necessary to circulate blood throughout the body. It is composed of three

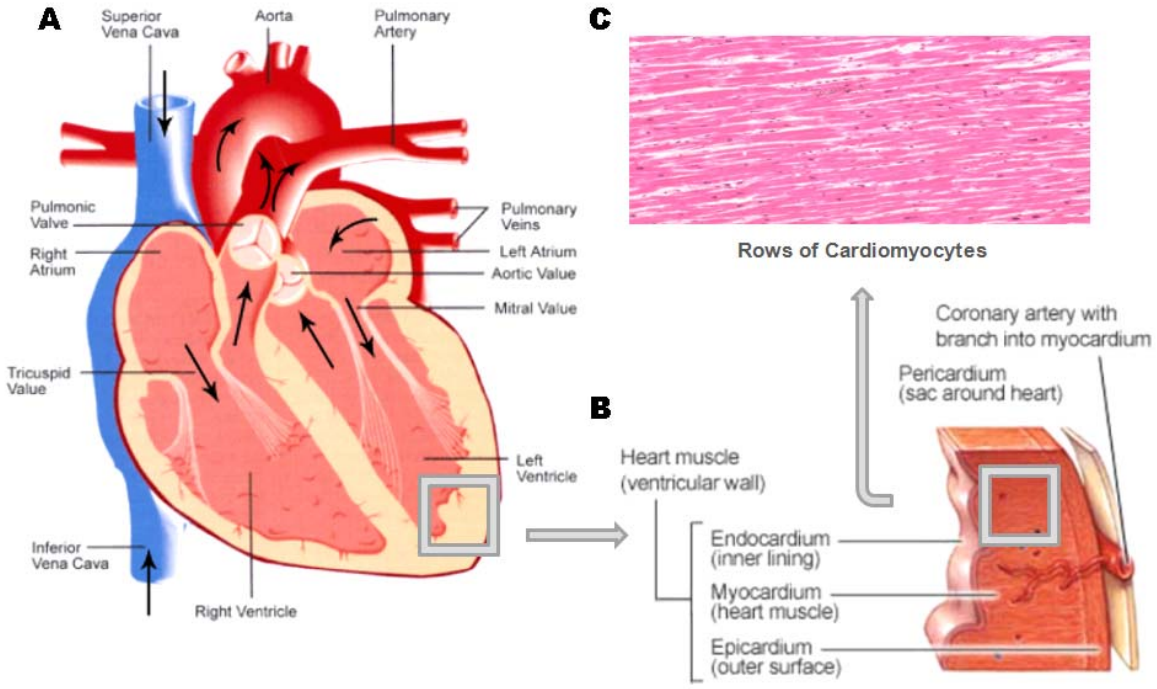

Figure 1. Cardiac anatomy and blood flow. (A) Blood returns to the heart through the superior and inferior vena cava, enters the right atrium and is pumped into the right ventricle. It then moves through the pulmonary arteries to the lungs, is reoxygenated, and flows into the left atrium through the pulmonary vein. The left ventricle fills, with additional blood being forced into the chamber through the mitral valve by the right atrium. Ventricular contraction then pushes the blood into the aorta and throughout the body (*arrows*, blood flow). (B) The myocardium lies between an inner epithelial layer (*endocardium*) and an outer connective tissue layer (*epicardium*), and consists of stacks of muscle cells known as cardiomyocytes. The myocardium is most dense in the left ventricle, as significant force is needed to drive blood through the body. (C) Rows of cardiomyocytes arrange in parallel to form the myocardium. Figures modified from various sources [2-4].

tissue layers: the endocardium, myocardium, and epicardium (Fig. 1B). The inner-most layer, the endocardium, consists of epithelial cells that make contact with blood entering the chamber. The myocardium (medial layer) is the location of the heart muscle cells responsible for contraction during systole. The outer layer is a protective tissue known as the epicardium. The myocardium represents the majority of the left ventricular wall, and is composed of layers of cardiomyocytes (heart muscle cells) running in parallel (Fig. 1C), connected cytoplasmically by channels known as gap junctions. Studying the

myocardium at the cellular level is essential to understanding the underlying pathologies involved in cardiomyopathies such as cardiac hypertrophy.

The major histological features of the cardiomyocyte include: 1) numerous rows of myofibrils consisting of segments of interdigitating myosin and actin filaments called sarcomeres (Fig. 2A); 2) a cytoplasmic membrane structure similar to endoplasmic reticulum (ER) known as the sarcoplasmic reticulum (SR); 3) invaginations of the

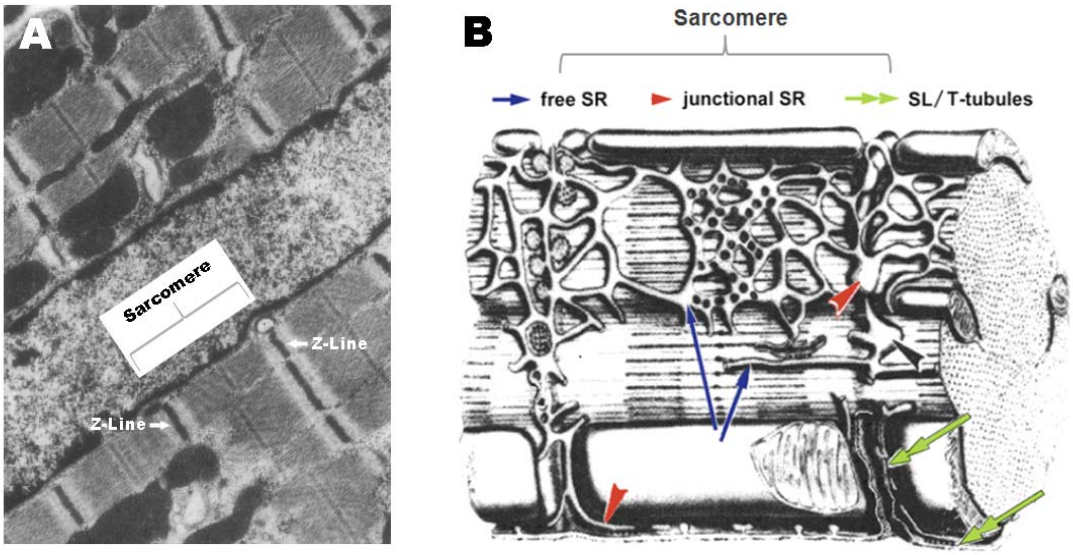

Figure 2. Myofibrillar structure. The main constituent of the cardiomyocyte is the myofibril. These long cylindrical structures themselves are made of many sarcomeres stacked in series, containing multiple types of contractile filaments. (A) An electron micrograph of the interior of a cardiomyocyte highlighting multiple myofibrils running in parallel. The sarcomere, the area between two Z-lines in a myofibril, is the contractile unit in the cell. (B) Myofibrils are wrapped in a network of endoplasmic reticulum-like compartments known as sarcoplasmic reticulum or SR. In the free SR, located between Z-lines, the Ca^{2+}-ATPase SERCA2a pumps Ca^{2+} into the SR network. The Ca^{2+} is then released at junctional SR located on Z-lines, through the ryanodine receptor after external Ca^{2+} entering through Ca^{2+} channels in the cell membrane (*SL*)/T-tubules triggers activation. Modified from Gottlieb et al. and Sommer et al. [5-6].

sarcolemma (cell membrane) called T-tubules; and 4) a large number of mitochondria running next to the myofibrils, to provide adequate ATP for cross-bridging termination and to fuel sarco/endoplasmic reticulum Ca^{2+}-ATPases (SERCA2a) [1, 7]. The

sarcomere, the most basic myofibril contractile unit, is bordered on both ends by Z-lines (Fig. 2A). Z-lines are the predominant sites of junctional SR, where SR membrane Ca^{2+} channels known as ryanodine receptors (RyR2) reside in close proximity to T-tubules that provide access to extracellular Ca^{2+} (Fig. 2B) [6].

The junctional SR/T-tubule interface is critical for cardiomyocyte contraction, as it is the site where calcium-induced calcium release (CICR) is initiated. Adjacent cardiomyocytes alter membrane potentials through gap junctions, leading to sarcolemmal depolarization, which causes L-type Ca^{2+} channels in T-tubules to open. The influxing extracellular Ca^{2+} binds the cytoplasmic side of junctional SR RyR2 channels which then open, allowing large quantities of SR Ca^{2+} to move into the cytoplasm. the Ca^{2+} subsequently binds troponin T, which releases tropomyosin bonds to actin and

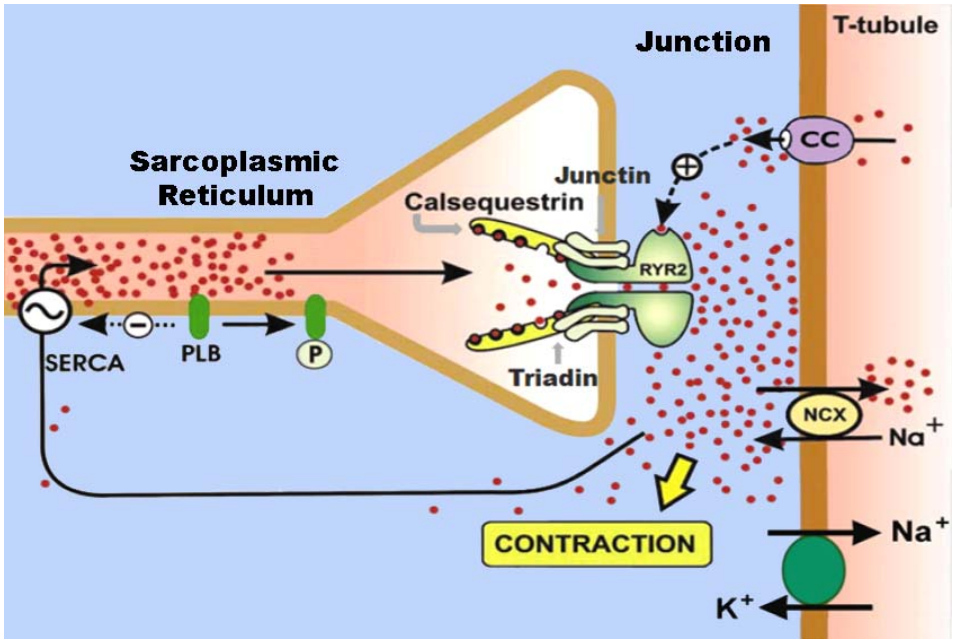

Figure 3. Calcium-induced calcium release. Depolarization of the heart cell membrane causes the L-type Ca^{2+} channel (*CC*) in the T-tubule to open, allowing Ca^{2+} to bind RyR2s located in the junctional SR membrane. The RyR2s then open, and Ca^{2+} moves into the cytoplasm, triggering contraction. Afterwards, Ca^{2+} is either pumped out of the cell by the Na^{+}/Ca^{2+} exchanger (*NCX*) or back into the SR by SERCA2a (*SERCA*), during which time CSQ2/Trd1/Jct complexes promote RyR2 refractory periods. Modified from Berridge et al. [8].

triggers contraction. Ca^{2+} is then either pumped out of the cell by the Na^{+}/Ca^{2+} exchanger (NCX) or back into the SR by SERCA2a, during which time cardiac calsequestrin (CSQ2), triadin-1 (Trd1), and junctin (Jct) theoretically interact to cause a RyR2 refractory period (Fig. 3) [8-9].

Calsequestrin

Calsequestrin (CSQ) is a major luminal protein of the junctional SR in muscle, where it is thought to play a role in excitation-contraction coupling [10-16]. While both skeletal CSQ (CSQ1) and cardiac CSQ (CSQ2) are expressed in skeletal muscle, only CSQ2 is present in cardiac muscle, where it is the major Ca^{2+} binding protein [17]. In fact, previous studies have hypothesized that nearly 50% of Ca^{2+} stored in cardiomyocyte SR is bound to CSQ2 [18], which is reasonable given its ability to bind large amounts of free Ca^{2+} (35-40 mol Ca^{2+}/mol CSQ2) [19-20]. CSQ2 shares structural properties with classic resident ER proteins such as GRP94 and calreticulin, although CSQ2 lacks the C–terminal KDEL retrieval sequence along with any other known targeting sequence [17, 21]. These properties allow CSQ2, through an unknown ER retention mechanism, to evade secretion and become concentrated in junctional SR [10-11, 16, 22]. Recent data supports the hypothesis that CSQ2 retention in ER results from its polymerization [23].

Enrichment of CSQ2 in secretory pathway compartments may be related to its tendency to polymerize in the presence of increasing Ca^{2+}. A model for Ca^{2+}-dependent CSQ polymerization has been developed based upon crystal structure, showing linear front-to-front and back-to-back CSQ chain formation [24-26]. As luminal SR Ca^{2+} levels increase, CSQ begins front-to-front polymerization due to the lesser charge on its N-

terminus. A further increase in Ca^{2+} causes back-to-back polymerization as more cations are needed to shield C-terminal acidic residues. High luminal Ca^{2+} levels eventually lead to the formation of CSQ linear polymers with front-to-front and back-to-back binding (Fig. 4) [26].

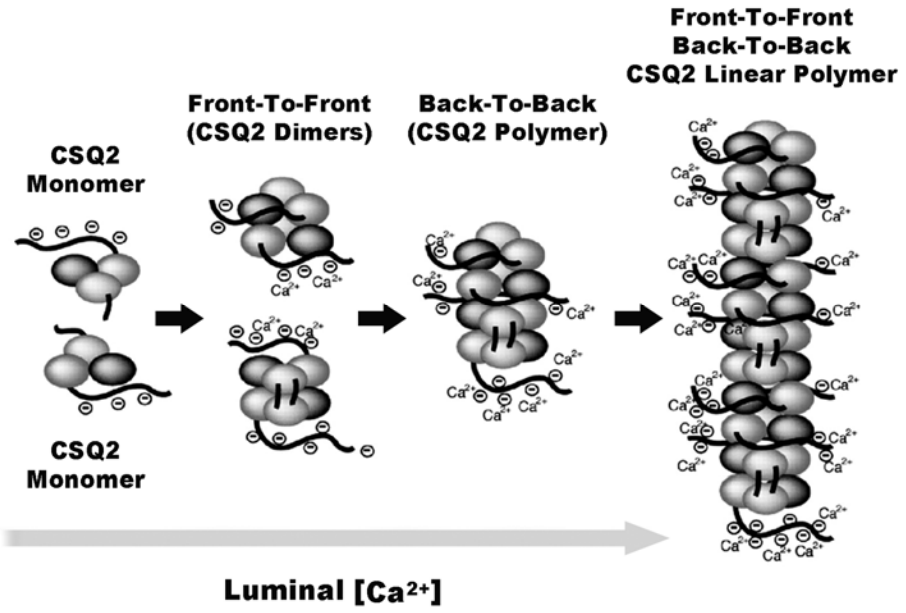

Figure 4. CSQ2 polymerization. As luminal SR Ca^{2+} levels increase, CSQ2 begins front-to-front polymerization due to the lesser charge on its N-terminus. Further increases in Ca^{2+} cause back-to-back polymerization as more cations are needed to shield C-terminal acidic residues. High luminal Ca^{2+} levels lead to formation of CSQ2 linear polymers with front-to-front and back-to-back binding. Modified from Park et al. [26].

In addition to its proposed function as an SR Ca^{2+} buffer, CSQ2 is also thought to interact with cardiac RyR2, the SR integral membrane protein responsible for supplying the cytosolic Ca^{2+} necessary for sarcomeric contraction. As proposed by Gyorke et al., CSQ2 serves as a Ca^{2+} sensor for the RyR2, promoting a channel refractory period in times of low luminal Ca^{2+} [9]. CSQ2 binds in low Ca^{2+} to either Trd1 or Jct, both of which may be tethered to the luminal side of the RyR2 in junctional SR. This is thought to inhibit RyR2 activity. As luminal Ca^{2+} concentrations increase, CSQ2 binds more Ca^{2+} and consequently becomes less tightly bound to Trd1 or Jct allowing stimulation of

channel activity. Eventually Ca^{2+} levels are high enough to cause CSQ2 dissociation from the complex, allowing the RyR2 to reach maximal activity (Fig. 5).

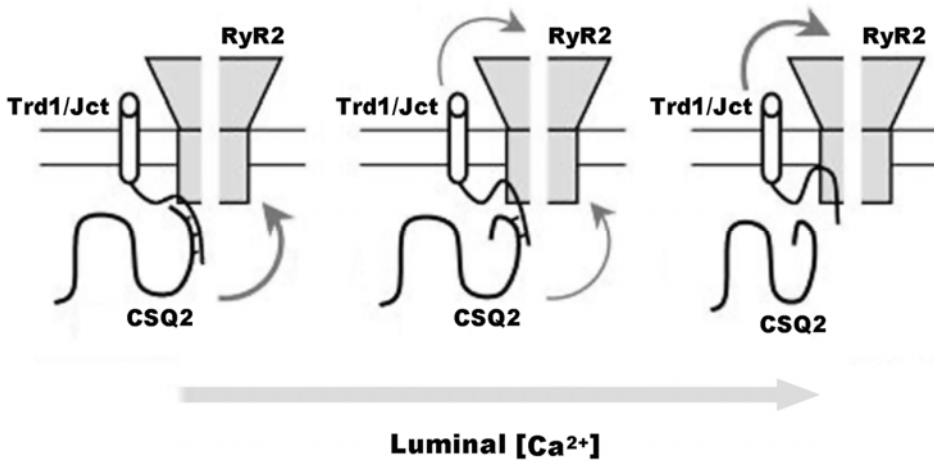

Figure 5. CSQ2 modulation of RyR2. CSQ2 is thought to serve as a Ca^{2+} sensor for the RyR2, promoting a refractory period for the channel in times of low luminal Ca^{2+}. CSQ2 binds to either Trd1 or Jct in low Ca^{2+}, inhibiting the RyR2. Increases in luminal Ca^{2+} concentration cause CSQ2 to become less tightly bound to Trd1/Jct allowing stimulation of channel activity. Eventually Ca^{2+} levels are high enough that CSQ2 dissociates from the complex and the RyR2 becomes maximally active. Modified from Gyorke et al. [9].

CSQ2-overexpressing and CSQ2-null transgenic mice have been developed in an attempt to determine CSQ2 protein function *in vivo* [27-28]. Overexpressing animals, with approximately 10-fold increases in cardiomyocyte CSQ2, suffer from severe hypertrophy causing heart mass and cell size to increase 2-fold [27]. In knockout mice, a hypertrophic phenotype was also reported, along with increased diastolic Ca^{2+} leak with pathology similar to a disease in humans caused by CSQ2 mutation, known as catecholaminergic polymorphic ventricular tachycardia (CPVT) [28-29]. Interestingly, both overexpression and knockout transgenic models show a significant decrease in Trd1 and Jct levels. Correspondingly, Trd1-null mice show a significant decrease in CSQ2 and Jct levels, highlighting a potential interdependence between the three proteins. A summary of the effects of CSQ2 knockout, along with Trd1-null data, can be

seen in Table 1, modified from Knollmann [30]. Because changes in CSQ2 levels are believed to be due to translational regulation [29], it would be beneficial to determine the

Table 1. Major features of CSQ2-null and Trd1-null mice.

	CSQ2-null	Trd1-null
1. Change in structure and SR protein composition:		
Cardiac hypertrophy	+	++
SR ultrastructure	Remodelled	Remodelled
SR volume	↑	No change
Number and extent of dyadic junctions	No change	↓ (50%)
RyR2 protein	No change	↓ (50%)
CSQ2 protein	0	↓↓
Triadin protein	↓↓	0
Junctin protein	↓↓	↓↓
SERCA2a protein	No change	No change
2. Change in function (baseline):		
Cardiac contractility in vivo	No change	↑
SR Ca^{2+} release	No change	↓
SR Ca^{2+} release fraction	↑	↓
SR Ca^{2+} content	Mild ↓ (14%)	↑
SERCA2a	No change	No change
3. Change in function after exposure to catecholamines (isoproterenol):		
SR Ca^{2+} leak	↑↑	↑↑
Occurrence of premature SR Ca^{2+} releases and triggered beats	↑↑	↑↑
SR Ca^{2+} content	↓	↑
Arrhythmia risk *in vivo*	↑↑	↑↑

site of CSQ2 synthesis.

Even without knowledge of the location of CSQ2 translation, it has still been possible to obtain data regarding trafficking pathways based upon electrospray ionization mass spectrometric analysis of the intact protein [31]. Information regarding CSQ2 trafficking results from the ability of mass spectrometry to visualize the entire repertoire of CSQ2 structures (glycoforms and phosphoforms) that exist in each experimental system [31-32]. An N-linked glycan is added to CSQ2 co-translationally (Man9GlcNAc2Glu3) in rough ER, and subsequently undergoes mannose trimming upon exposure to various secretory compartments and their respective mannosidases (Fig. 6) [31-32]. CSQ2 glycoforms differing in single mannose sugars (Δ162 Da) are easily discernable in CSQ2 mass spectra, allowing direct visualization of changes that

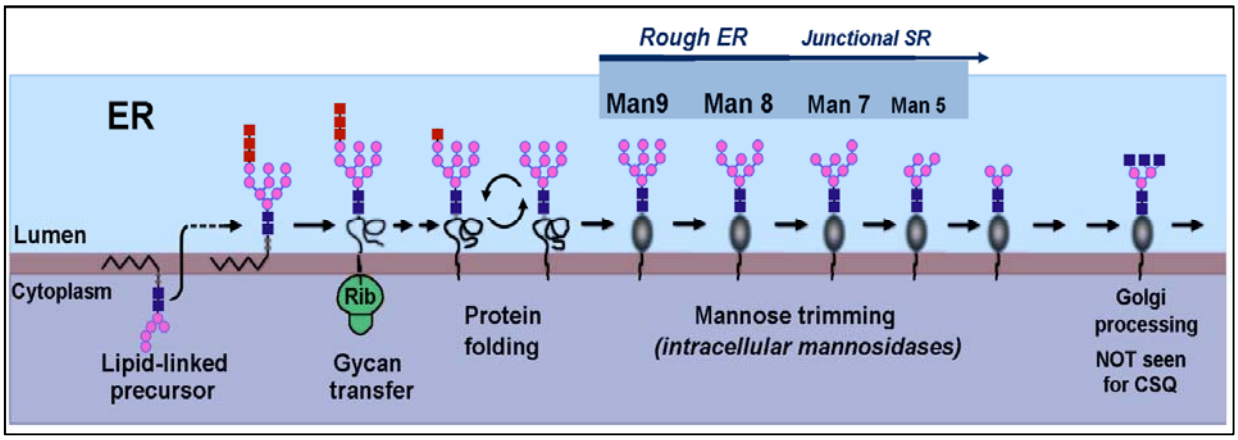

Figure 6. N-Linked glycosylation. The standard N-linked glycosylation pathway begins with co-translational transfer of the core oligosaccharide. Following successful folding of proteins in the ER, the glycan Man9GlcNAc2 remains intact. An ER mannosidase I produces the Man8 form. Subsequent mannose trimming is generally associated with ER and Golgi compartments, but this process has not been examined in heart. CSQ2 glycan does not contain N-terminal GlcNAc. Modified from Helenius et al. [32].

reflect trafficking pathways. A second important modification of CSQ2 is the phosphorylation of its multiple C-terminal serines (Fig. 7, in canine $^{378, 382, 386}$Ser) which can also be directly visualized (Δ81 Da). Between the possible combinations of mannose and phosphorylation states in CSQ2, twelve structural forms can be resolved from native heart tissue [31]; yet all will run in a nearly single band with SDS-PAGE analysis at approximately 55 kDa [33].

Based upon the distribution of CSQ2 glycan structures (Man9-Man1) in a normal mammalian heart, CSQ2 can be separated into two distinct pools [31, 34-35]. The most proximal glycoforms (Man9-6) also contain the highest levels of serine phosphorylation [31]; in fact all CSQ2 molecules in the heart that have 6 or more mannoses are also fully phosphorylated. This suggests that CSQ2 phosphorylation also occurs at a location early in the secretory system. A second pool is represented by Man1-5 isoforms. This second pool indicates further trafficking of CSQ2, but still represents trafficking that

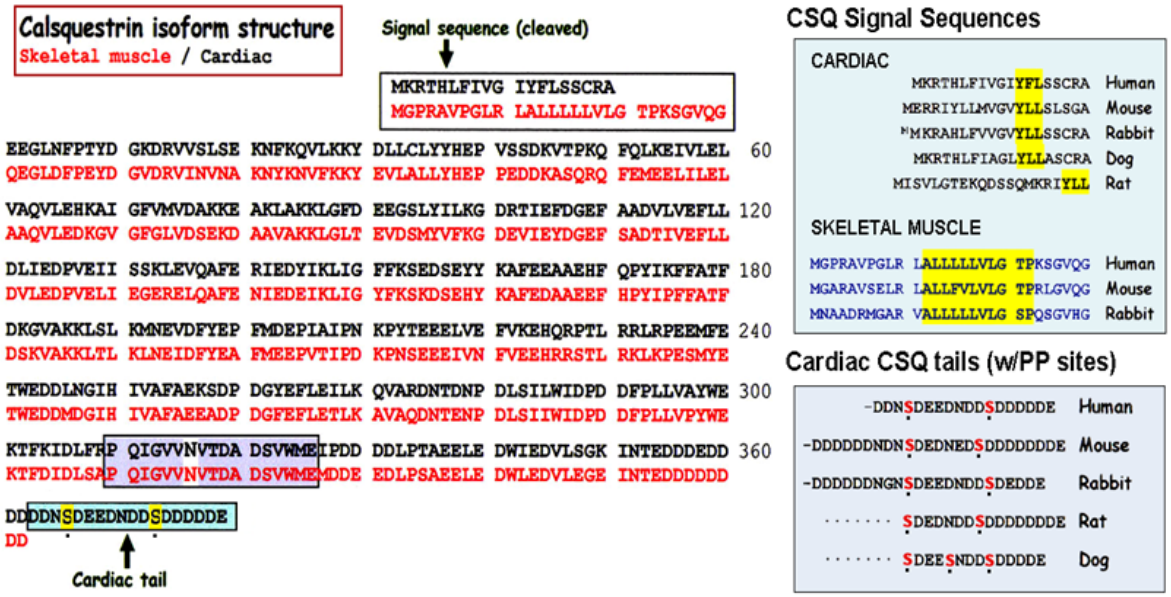

Figure 7. Features of CSQ sequences (sequences from NCBI database). (Left panel) Human cardiac (black) and skeletal muscle CSQ (red) sequences are 60% identical, and exhibit conserved glycosylation sites (2nd box from end of the full-length sequence). The cleaved signal sequences are very different, and that difference is conserved among species (upper right panel). Residues highlighted yellow are only examples of near identity, for orientation. The cardiac specific tail is seen in all species, and contains CK2-sensitive serine residues (indicated by black dots under the residues, in addition to yellow highlight in left panel, red lettering in lower right panel). Dotted lines for Rat and Dog C-termini (lower right panel) designate the fact that cardiac tail is uncertain, since skeletal muscle CSQ sequences have not been reported.

does not involve the Golgi, as Golgi trafficking would lead to addition of more (terminal) GlcNAc residues [31-32]. The second CSQ2 pool exhibits a lower level of phosphorylation, consistent with data using polymerization-site mutants that shows that the state of CSQ2 phosphorylation decreases with anterograde movement through the cell [23, 31, 34]. The distribution of glycoforms varies between cardiac and skeletal muscle CSQs. In skeletal muscle CSQ, Man1 (a highly unusual glycoform) represents as much as 80% of the total CSQ, while in cardiac muscle, CSQ2 Man1 levels are low with Man3,4 (species dependent) dominating [31, 34-35]. In contrast to CSQ2 in heart, CSQ2 overexpressed in nonmuscle cells consists of only Man9,8 glycoforms, indicative

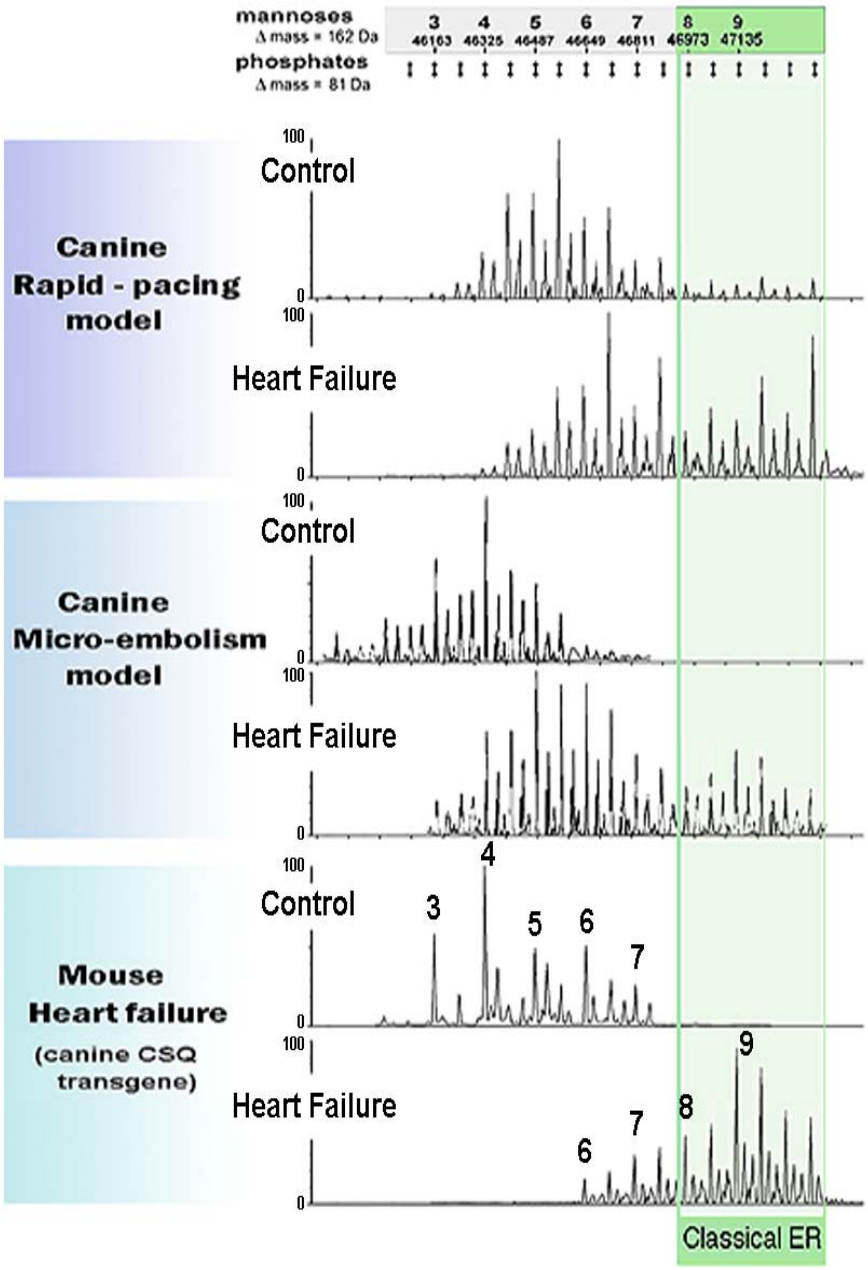

Figure 8. CSQ2 masses are altered in animal models of heart failure (HF). CSQ2 protein was purified from Control and Heart Failure animal heart, then directly analyzed by mass spectrometry. CSQ2 molecules from failed hearts were larger than CSQ2 from control hearts. Increased mass is due to reduced mannose trimming (Δ mass = 162 Da), indicative of a higher percentage of CSQ2 in early ER (*shaded)*. A second change is a decrease in more highly processed glycans. Mass heterogeneity also occurs due to C-terminal CSQ2 phosphates (Δ mass = 81 Da). Mass peaks and their corresponding glycan structure and phosphorylation state are indicated across the top of the figure. **(Canine rapid-pacing model)** tissue from five sham-treated and five HF dogs was provided by H. Valdivia, Univ. Wisconsin. Animals underwent ventricular pacing, (HF = 220 beats/min) for 6-8 weeks to induce heart failure. **(Canine micro-embolism model)** HF was caused by intracoronary microsphere injections leading to ischemic damage, tissue from H. Sabbah, Henry Ford Health Systems, Detroit, MI. These data were obtained from two Sham treated and two HF dogs, differences are more pronounced than in rapid-pacing. **(Mouse heart failure as a result of a canine CSQ2 transgene)** transgenic mice with an MHC-promoter driving canine CSQ2 overexpression have been previously characterized. Adult mice have severe heart failure and extreme cardiac hypertrophy. CSQ2 mass spectra were obtained from two cohorts of animals: only 4 transgenic mouse ventricles were needed to obtain sufficient CSQ2 for analysis, whereas 40 control mouse hearts were needed to obtain the Control mass spectrum. The glycan structure (GlcNAc2Man8,9) on CSQ2 from these animals is almost entirely indicative of ER mannosidase I, suggesting a completely altered trafficking.

of its highly efficient ER retention.

In heart tissue from a canine model of heart failure, CSQ2 glycoforms and phosphoforms are highly altered compared to control hearts (Fig. 8). Mass spectrometry of CSQ2 purified from these hearts shows a shift in the degree of mannose trimming to a less trimmed pool of molecules. The underlying cause of this apparent retrograde shift is unclear. Additionally, an approximate doubling of the Man8,9 pool occurred. This may suggest an increase in newly-synthesized CSQ2, still in rough ER. Analysis of CSQ2 mass spectra further indicates a doubling of maximally phosphorylated CSQ2, which could also reflect increased ER retention, or inhibition of the CSQ2 transport system [35].

CSQ2 phosphorylation and protein kinase CK2

In 1991, Cala and Jones reported a cluster of three phosphorylation sites on amino acids $^{378,\ 382,\ 386}$Ser of canine CSQ2 [36]. These phosphorylation sites reside within a cardiac specific tail region that is conserved in all cardiac isoforms in all species (Fig. 7). Cardiac CSQ is phosphorylated on these sites *in vivo* [31, 36], with isolated native CSQ2 showing approximately 50% phosphorylation. Skeletal muscle CSQ can be phosphorylated *in vitro* on ^{353}Thr but is not phosphorylated *in vivo* [31, 36]. It was subsequently determined that CSQ2 is the major substrate for endogenous phosphorylation in heart homogenate (Fig. 9) [34]. Surprisingly, CSQ2 overexpressed in nonmuscle cells is phosphorylated to a similarly high extent *in vitro* and in intact cells, suggesting that the mechanism of CSQ2 phosphorylation may be conserved in all mammalian cells [31]. While it has remained unclear what endogenous protein kinase is responsible for phosphorylating CSQ2 on these sites *in vivo*, these authors showed

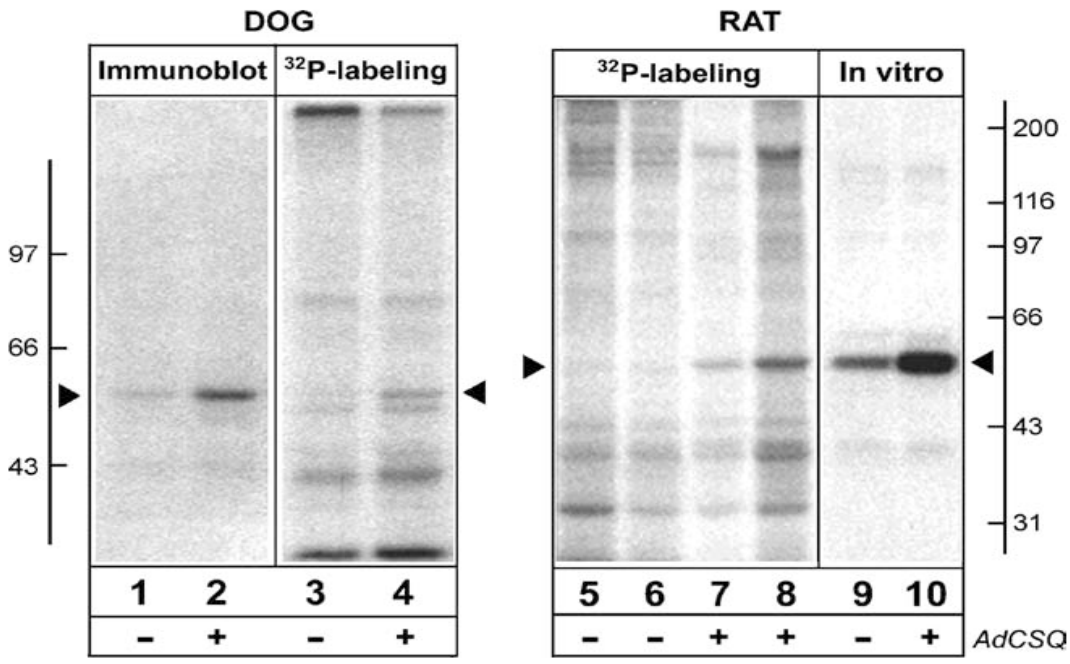

Figure 9. ***In situ*** **phosphorylation of CSQ2 by an unknown kinase.** Expression of canine CSQ2 in primary adult rat and canine heart cells was followed by metabolic labeling with $^{32}P_i$. Canine (lanes 1–4) or rat (lanes 5–10) heart cell cultures were plated in a laminin-coated sixwell dish. At 2 h post-plating, CSQ2 adenovirus (*Ad.CSQ*) was added (+), or cells were left untreated (−). In one case, a non-phosphorylatable CSQ2 mutant virus (Ad.nonPP) was added (lane 6). After 48 h of treatment, cells in two wells were harvested without labeling for immunoblot analysis with anti-CSQ2 antibodies, and visualized with ^{125}I-protein A and autoradiography (lanes 1 and 2). Cells in other wells (lanes 3–8) were metabolically labeled with $^{32}P_i$ in label-free medium (DMEM) for 4 h, harvested in 0.1% Triton X-100 containing buffer, centrifuged to remove insoluble material, and analyzed by SDS-PAGE and autoradiography. Molecular weight standards (in kDa) are indicated. Heart cells from five cultures were metabolically labeled for 4h (lane 3–7) whereas one sample was labeled for 8h (lane 8). Two culture wells (lanes 9 and 10) were not radiolabeled but were extracted in 0.5 ml 1% Triton X-100-containing buffer and 50 µl added to a buffer containing 1 mM MgCl2 and 20 µM [γ -^{32}P] ATP for 10 min at 37°C, before SDS-PAGE and autoradiography. Arrowheads indicate CSQ2. Modified from Ram et al. [34].

that the sites were very sensitive *in vitro* to the protein kinase CK2 (formerly known as casein kinase II). Moreover, the phosphorylation sites are part of a consensus sequence for CK2.

A basic structural requirement for phosphorylation by CK2 is the "serine/threonine-X-X-aspartic acid/glutamic acid" motif [37-38]. The fourteen most C-terminal amino acids of canine CSQ2's highly acidic tail, **S**DEE**S**NDD**S**DDDDE,

includes three serines that fit the consensus sequence [33, 36]. Although CSQ2 is an SR luminal protein, and protein kinase CK2 is known to be a cytosolic or nuclear kinase [39], an unknown mechanism must exist that allows for CSQ2 consensus site exposure to CK2.

Over 500 protein kinases are represented by the human genome [40]. While protein kinase CK2 is only one of many, it is one of the more active kinases in numerous cell-types [41-42]. CK2 has been reported to phosphorylate hundreds of distinct proteins, positively affecting cell proliferation/cell cycle progression and survival by means of apoptotic inhibition and other various mechanisms [39, 41, 43-46]. Protein kinase CK2 has become the focus of many oncological studies as levels have been found to be elevated in human cancers and in transgenic overexpression models [41, 47-49].

Although CK2 is traditionally thought of as a holoenzyme, its biochemistry is slightly more complex. CK2 is a tetrameric structure consisting of two catalytic and two regulatory subunits [41, 44, 50]. The catalytic subunits, designated CK2α and CK2α′ in humans [51], share approximately 90% homology [41], but may possess some level of specialization as suppression of one subunit in mouse models does not produce a complete compensation by the other [44, 52]. The regulatory subunits, known as CK2β, participate in catalytic activity regulation and CK2 substrate selectivity, in addition to maintaining tetramer stability during holoenzyme formation [41, 44, 50, 53]. CK2 regulatory subunits are identical in humans, performing equal roles [54], while they have been reported to have separate identities in yeast where they are both essential [55]. To further complicate protein kinase CK2 research, an overall mechanism has not been

deduced that summarizes the regulation of the kinase in cells; as some groups argue that CK2 is constitutively active while others claim the influence of extracellular or intracellular factors exists [41].

In addition to phosphorylating substrate as part of the holoenzyme, the individual catalytic subunits CK2α and CK2α′ also have kinase activity independent of the tetramer [56-57]. For example, both the holoenzyme and CK2α subunit were shown to phosphorylate the cytosolic region of calnexin, a protein that shares many similarities with CSQ2 [56]. Interestingly, both catalytic subunits have been shown to localize to the cytosolic side of the ER and Golgi apparatus [57]. This data, collectively, suggests that CK2 function and regulatory activity is quite complex and will require many future studies to explain.

Highly specific inhibitors of CK2 have recently been developed and continue to be improved due in part to the desirable anti-growth and anti-cancer activities they exhibit [58-59]. The three main classes of CK2 inhibitors include: 1) condensed polyphenolic compounds; 2) brominated benzimidazole/triazole derivatives; and 3) derivatives of indolo quinazolines. The second class is the most frequently and successfully used [60]. The first of these ATP specific binding-site inhibitors of CK2, 5,6-dichloro-1-(β-ᴅ-ribofuranosyl)-benzimidazole (DRB), was designed as a modified version of adenosine. Due to high experimental IC_{50} values and various off-target effects, the popular DRB derivative 4,5,6,7-tetrabromobenzotriazole (TBB, Fig. 10) was created by removing the sugar moiety and replacing its chlorines with bulkier bromines. TBB was determined to be more potent and selective than DRB, and was also well tolerated in live animals for multiple week spans [61]. A slightly modified version of

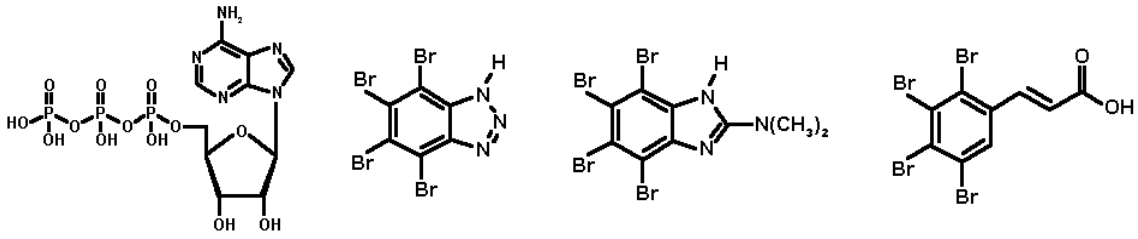

Figure 10. Development of CK2 inhibitors. Inhibitors of protein kinase CK2 were initially designed to mimic ATP structure. The specific inhibitor TBB was created to better fit the unique ATP binding site of CK2. TBB was modified to produce DMAT, increasing the molecules potency. TBCA represents the most potent and specific of this class of ATP-competitive binding site inhibitors of CK2. Modified from Duncan et al. and Sarno et al. [61, 63].

TBB, 2-dimethylamino-4,5,6,7-tetrabromo-1H-benzimidazole (DMAT, Fig. 10) was found to have an even higher potency, particularly when tested on cells in culture [62]. Currently, tetrabromocinnamic acid (TBCA, Fig. 10), the most specific CK2 inhibitor in its class, has the lowest K_i (77 nM) [61]. It is thought that TBCA's acrylic tail increases van der Waals interactions, as it allows the brominated benzene ring to move [60].

Translation and translocation

Translocation of a newly translated protein into the ER lumen can occur after translation is completed or concurrently with translation. The latter is referred to as co-translational translocation. During this process, signal sequences within a nascent polypeptide are recognized by universally conserved factors in the cytosol and membrane in order to mediate their selective targeting, translocation, and/or membrane insertion (Fig. 11A) [64]. These events proceed when the hydrophobic core of the signal sequence from the newly-synthesized protein protrudes from the ribosome and becomes bound by the signal recognition particle (SRP), forming the SRP-bound ribosome nascent chain complex (RNC). Interaction with the SRP receptor (SRP-R)

allows the RNC to be targeted to the ER membrane, where it is then transferred to an adjacent translocon followed by subsequent dissociation of the receptor-bound SRP complex via GTP consumption. The ribosome binds to the Sec61 complex (Fig. 11B), placing the signal sequence in close proximity to the translocating chain-associating membrane protein (TRAM) and Sec61. If the signal sequence is recognized sufficiently by the Sec61 complex, nascent chain insertion into the hydrophilic pore occurs with a concurrent tightening of the bond between the ribosome and translocon. After further elongation of the nascent chain, with its simultaneous translocation into the ER, it can interact with the oligosacharyl transferase complex (OST) and signal peptidase complex

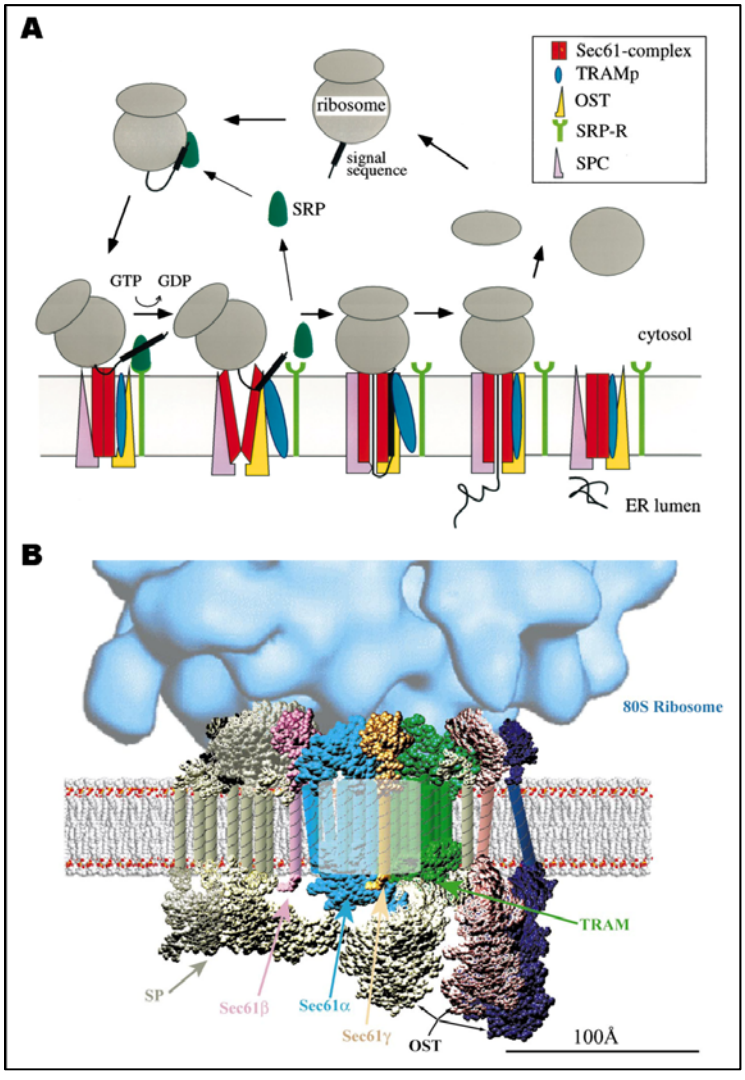

Figure 11. Co-translational translocation. (A) As translation begins, the nascent chain signal sequence protrudes from the ribosome and is bound by SRP. The complex is then trafficked to an ER translocation site where SRP is bound by the SRP receptor and the ribosome binds to the Sec61 pore complex. SRP hydrolyzes GTP and releases from the signal sequence, ribosome, and eventually the SRP receptor, leaving the signal sequence to interact with Sec61 and TRAM complexes. The nascent chain is then further synthesized while being translocated into the ER lumen, possibly receiving a glycan from the OST complex and/or having its signal sequence removed by the SPC. (B) A to scale depiction of the rough ER translocon showing theoretical spacial approximations of various complexes according to their interactions with one another (*SP*, signal peptidase). Modified from Johnson et al. and Kalies et al. [65-66].

causing glycosylation and signal sequence cleaving, respectively, given the nascent chain sequence permits [64, 66].

In part due to their extreme sequence diversity, it has been proposed that signal sequence interaction with Sec61 is influenced by the signal's intrinsic ability to attract specific translocaton altering substrates, termed accessory factors [64]. These modulators (accessory factors) can include membrane proteins, cytosolic proteins and luminal proteins, i.e. chaperones. These substrates allow for proper positioning of the nascent chain in preparation for subsequent translocation.

A universal property of signal sequences is their overall hydrophobic nature, highlighted by the presence of an uninterrupted stretch of no less than six nonhydrophilic residues [64]. When a comparison of signals is made between cardiac and skeletal calsequestrin isoforms from various species, it can be noted that the hydrophobic core is much more significant in skeletal muscle (Fig. 7). This difference in hydrophobicity can affect interactions with the translocon apparatus [64], and may contribute to the ability of cardiac calsequestrin to become phosphorylated during translocation.

Significance

CSQ2 is capable of binding large amounts of Ca^{2+} within the secretory system in cardiomyocytes. It is also thought to regulate RyR2 activity in junctional SR. Previously published data shows that CSQ2 trafficking is altered in heart failure. A change in CSQ2 localization within the cell could result in a significant Ca^{2+} microdomain shift, capable of altering cellular biochemistry. In order to investigate this pathological phenomenon properly, the site of CSQ2 synthesis, and the protein's subsequent

trafficking pathway must first be elucidated. Additionally, possible effectors of CSQ2 trafficking, such as polymerization and phosphorylation, must be explored.

SPECIFIC AIMS OF DISSERTATION

Specific aim 1

Determine the pathway(s) of CSQ2 trafficking in the adult cardiomyocyte. Hypothesis: CSQ-DsRed fusion protein exhibits retention in rough ER and reflects normal CSQ2 trafficking pathways, involving polymerization.

Specific aim 2

Confirm the identity of CSQ2 kinase and determine the effects of CSQ2 phosphorylation. Hypothesis: CSQ2 is phosphorylated by protein kinase CK2, which may affect its ER-retention.

CHAPTER 2

EFFECTS OF A DYNAMIC MONOMER/POLYMER EQUILIBRIUM ON CARDIAC CALSEQUESTRIN TRAFFICKING

ABSTRACT

CSQ2 is synthesized in rough ER but concentrates within the junctional SR lumen where it becomes part of the Ca^{2+}-release protein complex. To investigate CSQ2 trafficking through biosynthetic/secretory compartments of adult cardiomyocytes, CSQ-DsRed was overexpressed in cultured cells and examined using confocal fluorescence microscopy. By 48 h of adenovirus treatment, CSQ-DsRed fluorescence had specifically accumulated in the nuclear envelope, where it co-localized with markers of rough ER. From rough ER, CSQ-DsRed appeared to traffic directly to junctional SR along a transverse (Z-line) pathway along which sec 23-positive (ER-exit) sites were enriched. In contrast to DsRed direct fluorescence that presumably reflected DsRed tetramer formation, both anti-DsRed and anti-CSQ2 immunofluorescence did not detect the perinuclear CSQ-DsRed protein, but labeled only junctional SR puncta. These putative CSQ-DsRed monomers, but not the fluorescent tetramers, were observed to traffic anterogradely over the course of a 48 h overexpression from rough ER towards the cell periphery. We propose a new model of CSQ2 and junctional SR protein trafficking in the adult cardiomyocyte, wherein CSQ2 traffics from its juxtanuclear site of biosynthesis, along contiguous ER/SR lumens in cardiomyocytes as a mobile monomer, but is retained in junctional SR as a polymer.

INTRODUCTION

CSQ2 is a major protein of the junctional SR lumen in heart [11, 17, 67]. Its role

in cardiomyocyte function is not yet clear, and may be multi-faceted [30, 68-69]. Overexpression studies in cultured myocytes support a role as a buffer of luminal Ca^{2+} [13], whereas data from CSQ2 knockout mice suggest a role in regulation of release of Ca^{2+} through the RyR2 Ca^{2+} channel [28]. Interestingly, transgenic CSQ2 overexpressing [27] and knockout mouse models [28], also exhibit unexplained changes in the levels of other junctional SR proteins, such as Trd1, Jct, and RyR2. These larger changes in junctional SR protein levels highlight our poor understanding of the biosynthetic/secretory system of the adult cardiomyocyte, of which ER, free SR, and junctional SR are all a part [70].

Polymerization of CSQ is now thought to play a critical role in its biology, and is predicted to occur in response to high luminal ER/SR Ca^{2+} [26, 68-69]. Although difficult to study in myocytes, studies of CSQ2 overexpression in nonmuscle cells have clearly shown how polymerization can also determine CSQ2 localization [23, 71-72]. In mammalian nonmuscle cells, each CSQ isoform (cardiac or skeletal muscle) undergoes polymerization that leads to its concentration in a specific cellular compartment. Cardiac CSQ concentrates exclusively in the ER of all nonmuscle cells, whereas skeletal muscle CSQ concentrates in the ER-Golgi intermediate compartment (ERGIC). The distinct sites of localization for the two CSQ isoforms were the result of their specific polymerization properties [71]. In this same way, polymerization of cardiac CSQ in adult cardiomyocytes might occur specifically in junctional SR puncta, brought about by the ionic milieu of junctional SR lumens.

Another biochemical property of cardiac CSQ that is likely to play a role in its biology is phosphorylation on two or more serines in the cardiac-specific tail [31, 34, 36].

These C-terminal protein kinase CK2 consensus sequences are present in all cardiac isoforms of CSQ and are exquisitely sensitive to CK2 *in vitro*. This modification is believed to occur at the rough ER of the cardiomyocyte where it may affect CSQ2 translocation or CSQ2 trafficking from rough ER to junctional SR [34]. CSQ2 glycans show trimming by cellular mannosidases with no other modification. Because N-acetyl glucosamine (GlcNAc) would be found on CSQ2 glycans were CSQ2 to traffic to early Golgi compartments [23, 73], it becomes likely that CSQ2 remains inside classical mammalian ER.

In a canine tachycardia-induced model of hypertrophy that leads to heart failure, CSQ2 glycosylation and phosphorylation are very significantly altered [35]. CSQ2 glycan structures in the hypertrophic heart show a two-fold increase in ER-localized CSQ2 and a roughly two-fold increase in levels of phosphorylated CSQ2 in the ER [35]. The cellular processes underlying these changes have remained uncertain due to the lack of understanding of CSQ2 biosynthesis and trafficking in the adult cardiomyocyte.

In the present study, we used confocal imaging techniques to investigate the direct fluorescence of CSQ-DsRed along with a complementary indirect immunofluorescence, to outline ER and SR regions in adult cardiomyocytes that parallel putative CSQ2 compartmentation based upon on its biochemistry.

MATERIALS AND METHODS

Heart cell preparation and culture

This investigation conforms with the *Guide for the Care and Use of Laboratory Animals* published by the US National Institutes of Health (NIH Publication No. 85-23, revised 1996). Animal research was approved by the Wayne State University Animal

Investigation Committee (protocol # A 06-07-07). Excised Sprague-Dawley (*Rattus norvegicus*) rat hearts were perfused using a Langendorff apparatus for 5 min before enzymatic dissociation using a 40 ml solution consisting of Liberase Blendzyme (Roche) types 1 and 2 (3 mg/6 mg) in Hank's buffer containing 5 mM pyruvic acid, 1.2 mM $MgSO_4$, 5 mM creatine, 11 mM Glucose, 5 mM taurine, 5 mM carnitine and 0.1 mM $CaCl_2$ (20 min). Cells were titurated for 10 min at 37ºC, filtered, pelleted at 300 x g_{max}, then washed in phosphate buffered saline (PBS) containing gradually increasing $CaCl_2$ during 3 consecutive washes, to a concentration of 500 μM $CaCl_2$, after which cells were resuspended in Medium 199 containing 2% bovine serum albumin, 2 mM carnitine, 5 mM creatine, 5 mM taurine, 2 mM L-glutamine, 2 mM Glutamax-1 (Invitrogen), ITS mixture (Sigma I3146), 100 units/ml penicillin G, 0.1 mg/ml streptomycin and plated on laminin-coated dishes at 37ºC with 5% CO_2.

CSQ plasmid and adenoviral constructs

CSQ constructs were generated from wild type canine cardiac CSQ cDNA λgt10 clone IC3A [33]. Adenoviral CSQ-DsRed (Ad.CSQ-DsRed) was created using the AdEasy XL Adenoviral Vector System (Stratagene) after canine cardiac CSQ cDNA had been cloned into pDsRed2-N1 vector as previously described [71]. Adenoviral CSQ-hemagglutinin (Ad.CSQ-HA) was previously described [23].

Adenoviral-mediated overexpression

Recombinant adenoviral treatment was carried out in cultured adult rat primary cardiomyocytes as previously described [31]. Adenoviruses were added directly to dishes 2 h post-plating at a multiplicity of infection (MOI) of 100. Virus treatments were routinely carried out for 48 h before harvesting for biochemical analysis or fixing for

microscopy as described below. Individual dishes and coverslips were incubated for shorter or longer times as indicated.

Antibodies

Monoclonal antibodies specific to cardiac CSQ and RyR2 were the generous gift of Dr. Larry Jones, Indiana University School of Medicine. Rabbit polyclonal antibodies raised to canine CSQ2 were purchased from Abcam (ab3516). Rabbit polyclonal anti-HA antibody was purchased from Sigma-Aldrich. Rabbit polyclonal anti-sec23 antibody was obtained from Affinity BioReagents. Rabbit polyclonal anti-DsRed antibody was purchased from Clontech. Rabbit polyclonal antibodies specific to translocon-associated protein complex (TRAP) and translocating chain-associated membrane protein (TRAM) were the generous gift of Dr. Ramanujan Hegde, National Institute of Child Health and Human Development, NIH. Alexa Fluor 488-conjugated goat anti-rabbit IgG, Alexa Fluor 488-conjugated goat anti-mouse IgG and Alexa Fluor 568-conjugated goat anti-mouse IgG secondary antibodies were purchased from Invitrogen.

Immunoblotting

SDS-PAGE was carried out according to Laemmli [74] on 7.5% acrylamide gels, transferred to nitrocellulose membranes (0.45 μm, Bio-Rad Laboratories) and stained with Amido black (Sigma). Immunoblotting was carried out as previously described [42] using HRP-coupled secondary antibodies. Horseradish peroxidase (HRP)-conjugated goat anti-rabbit IgG and goat anti-mouse IgG secondary antibodies were obtained from Jackson ImmunoResearch Laboratories. A SuperSignal West Pico Chemiluminescent Substrate (Thermo Scientific) electrochemiluminescence (ECL) kit was used according to the manufacturer's protocol to detect immune complexes, which were then visualized

by autoradiography using Amersham Hyperfilm ECL film (GE Healthcare). Protein concentrations were determined according to Lowry [75].

Fluorescence microscopy

Cells were fixed on coverslips with 4% paraformaldehyde in PBS for 10 min and then permeabilized for 5 min in 0.2% Triton X-100. Coverslips were blocked in PBS with 0.2% Tween-20 (PBS/Tween) and 2% goat serum at room temperature for 1 hour. Cells were then incubated in PBS/Tween with primary antibody (1:200) for 90 min at ambient temperatures, followed by washing in PBS/Tween, and incubation with goat anti-rabbit IgG or goat anti-mouse IgG antibodies conjugated to Alexa Fluor dyes (1:500 dilution in PBS/Tween for 60 min). Cells were counterstained with 100 μM 4′-6-diamidino-2-phenylindole (DAPI) for 2 min, rinsed, and mounted to microscope slides with ProLong Antifade Mounting Kit (Molecular Probes). Confocal microscopy was performed at the Microscopy and Imaging Resources Laboratory at Wayne State University, School of Medicine. Imaging was performed using a C-Apochromat 63x/1.2 WKorr water objective on either a Zeiss LSM 510 laser scanning microscope or an Axioplan2 Imaging fluorescent microscope with Apotome imaging, or using a 63x/1.4 oil objective on a Leica TCS SP5 laser scanning microscope. Laser scanning images were acquired on a 1024 x 1024 pixel canvas with 8-line averaging. Apotome images were obtained with a Zeiss Axiocam MRm B/W CCD camera. Confocal images were processed and optimized offline for publication using Photoshop (Adobe Systems Inc.). Z-stack images created by the Leica TCS SP5 were compiled and optimized in ImageJ (Wayne Rasband, National Institutes of Health). The ImageJ 3D Viewer plugin was used to create three-dimensional z-stack images.

RESULTS

CSQ-DsRed is localized to perinuclear regions of the cardiomyocyte

Following its overexpression in cultured adult rat cardiomyocytes, the fluorescent fusion protein CSQ-DsRed produced a unique pattern of subcellular localization in which both myonuclei were surrounded by intense red fluorescence (Fig. 12). Red fluorescence could be visualized in most cells after 32 h of virus treatment, consistent with levels of overexpression observed by immunoblotting (Fig. 13). CSQ-DsRed accumulated in cardiomyocytes to levels that were comparable to endogenous levels of CSQ2 after 48 h, by which time CSQ-DsRed prominently surrounded both nuclei

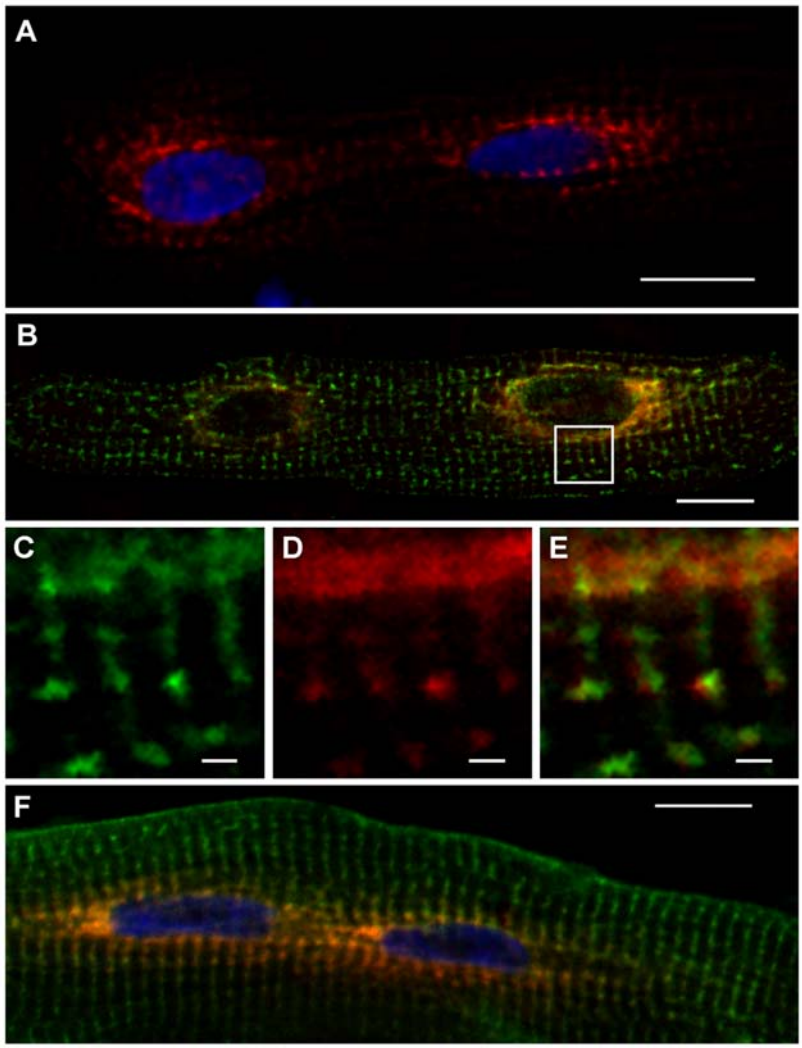

Figure 12. Perinuclear localization of CSQ-DsRed in cultured adult rat cardiomyocytes. (A) Cultured primary adult rat cardiomyocytes plated on glass coverslips were treated with Ad.CSQ-DsRed for 48 h, and DsRed fluorescence was analyzed by confocal fluorescence microscopy after fixation. (B) Cells treated with Ad.CSQ-DsRed (red) were stained with anti-RyR2 antibodies (green). Enlarged area (*white box* in panel B) shows RyR2 immunostaining (C) or CSQ-DsRed fluorescence (D). (E) a merge of C and D, shows imperfect co-localization of CSQ-DsRed and RyR2. (F) Cells co-infected with Ad.CSQ-DsRed (red) and Ad.CSQ-HA (green) were stained with anti-HA antibodies. Bars, 20 μm (panels A,B,F) or 2 μm (panels C,D,E). Imaging, Apotome (panels A,F), Leica, (panels B-E).

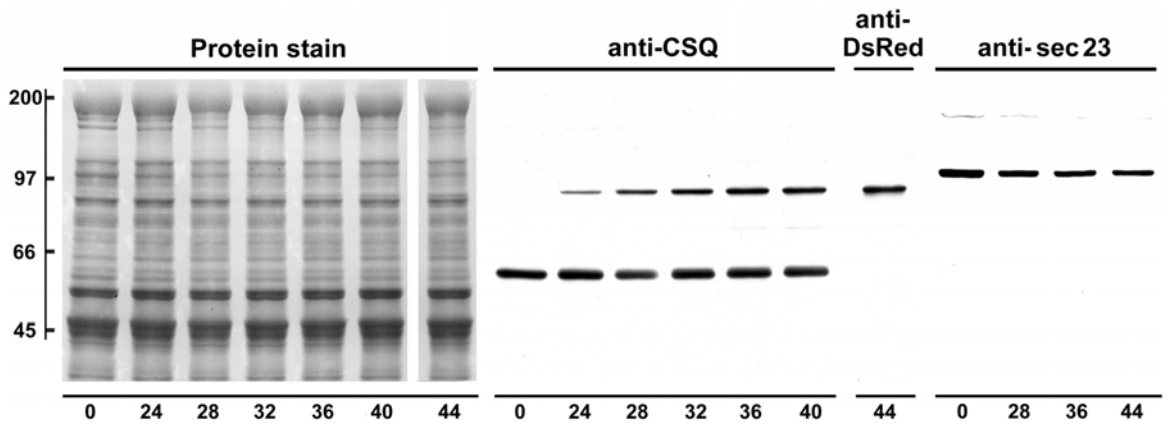

Figure 13. Immunoreactivity and specificity of anti-CSQ2, anti-DsRed, and anti-sec23 antibodies examined by immunoblotting as a function of CSQ-DsRed overexpression. Following addition of Ad.CSQ-DsRed, cardiomyocytes were cultured for indicated times (24-44 h). Cells prior to adenovirus treatment are shown as t = 0. Cells were harvested in SDS-containing buffer and whole cell homogenates (equal volumes from each cardiomyocyte dish, roughly 80 µg) were analyzed by SDS-PAGE and immunoblotting. The nitrocellulose membrane was stained with amido black (Protein stain), then probed with either anti-CSQ2 (t = 0, 24-40 h), anti-DsRed (t = 44 h), or anti-sec23 antibodies. Mobilities of molecular weight standards in kDa, left margin.

producing a pattern that was qualitatively similar for hundreds of cells examined. We observed a very similar pattern of CSQ-DsRed localization in dishes of live (unfixed) cultured cardiomyocytes (data not shown). In addition to a very high level of red fluorescence that appeared in close apposition to the nucleus, CSQ-DsRed could be seen, albeit with much lower intensity, in perinuclear puncta. At these sites, the pattern of CSQ-DsRed fluorescence was similar (Fig. 12C,D) but not identical (Fig. 12E) to RyR2-positive immunofluorescence. Peripheral CSQ-DsRed puncta became more apparent with increasing time of virus treatment in culture, or when images were brightened offline. In contrast to the peculiar CSQ-DsRed localization, the CSQ2-fusion protein CSQ-HA was uniformly present in puncta throughout the cell, and never exhibited the perinuclear enrichment observed using CSQ-DsRed (Fig. 12F). This suggested that the concentration of perinuclear CSQ-DsRed had resulted from the

characteristic tetramerization of the DsRed portion of the fusion protein [76-77].

CSQ-DsRed around the nucleus co-localizes with rough ER markers

We hypothesized that the localization of CSQ-DsRed around the nucleus represented its site of biosynthesis, that is, cardiac rough ER. To determine whether markers of rough ER supported the juxtanuclear localization of cardiac rough ER, we immunostained cultured cardiomyocytes with antibodies against components of the protein biosynthesis and translocation machinery. TRAP is a major protein component of the translocon in mammalian cells, where it is involved in nascent protein translocation across the rough ER membrane [78]. Indirect immunofluorescence of the subunit TRAPα in cultured cardiomyocytes expressing CSQ-DsRed strongly labeled the

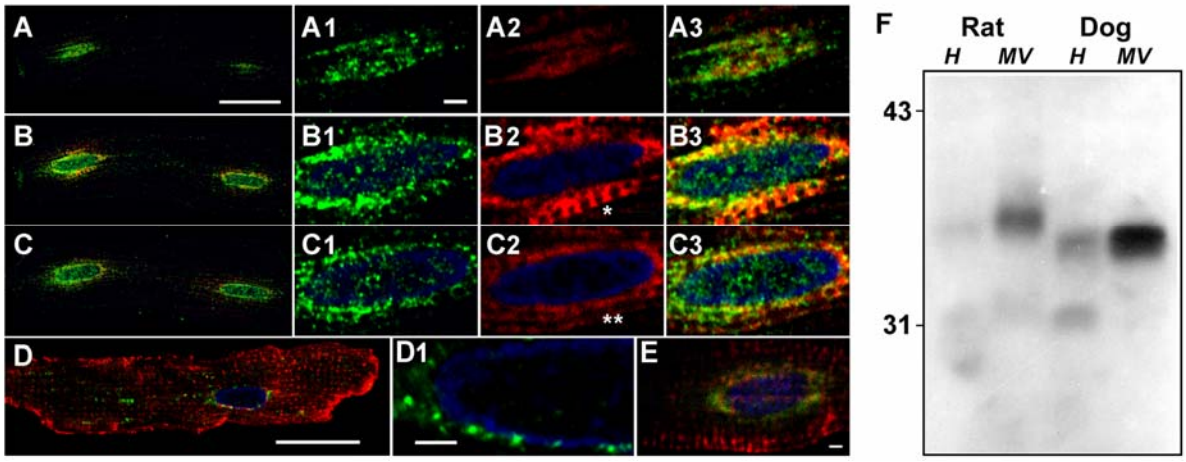

Figure 14. Labeling of the cardiomyocyte rough ER using classic rough ER markers. Cardiomyocytes were treated with CSQ-DsRed adenovirus for 48 h (red, A-C,E). Anti-TRAPα images (green) were acquired from three optical planes starting from atop the nucleus (A), and 2.2 μm (B) or 4.4 μm (C) below (bar, 20 μm). Panels 1-3 (TRAPα, CSQ-DsRed, merge, respectively) are enlargements of the leftmost nucleus of each cell shown in A-C (bar, 2 μm). Transverse trafficking of CSQ-DsRed can be seen in the optical plane that dissects the nuclear midline (B2, *asterisk*) but appears as distinct cisternae in an adjacent optical slice (C2, *double asterisk*). Anti-TRAM immunofluorescence (green) was imaged in cardiomyocytes not treated with Ad.CSQ-DsRed, but immunostained with ant-RyR (red): D1, rightmost nucleus in panel D. Bar, 2 μm. (E) anti-ribosomal S6 protein immunofluorescence (green) was imaged in cells overexpressing CSQ-DsRed (red). Bar, 2 μm. Imaging, Leica (panels A-D), Zeiss LSM (panel E). (F) immunoblot analysis of rat and dog heart homogenates (H, 100 μg) and microsomal vesicles (MV, 50 μg) using anti-TRAPα antibodies. Mobilities of molecular weight standards in kDa, left margin.

myocyte perinuclear region, co-localizing with CSQ-DsRed fluorescence (Fig. 14A-C). Levels of anti-TRAPα immunofluorescence were highest in cisternae closely apposed to the nucleus, whereas CSQ-DsRed could be seen in selected optical slices to extending beyond to successive cisternae (panel C2, *double asterisk*). A single optical slice was sometimes able to capture transverse trafficking as a continuous CSQ-DsRed fluorescence between the perinuclear region and an adjacent cisterna (panel B2, *asterisk*). The abundance of TRAPα in cardiomyocyte membranes was also evident by immunoblotting, where it appeared as a single immunoreactive protein band of roughly 34 kDa [79] enriched in microsomes prepared from either rat or canine heart tissue (Fig. 14F). Further support for the idea that the perinuclear region could be a major site of protein synthesis in cardiomyocytes came from localization of the translocon accessory protein TRAM [80] and the ribosomal S6 protein (Fig. 14D,E *respectively*) to areas surrounding the myonucleus.

Transport of proteins from the rough ER in mammalian cells is associated with the formation of ER exit sites that become COPII transport vesicles [81-83]. Because fluorescence microscopy of CSQ-DsRed suggested a relatively direct transport step between its apparent site of biosynthesis (perinuclear rough ER) and adjacent junctional SR puncta, we asked whether ER exit site location might also reflect such transport in cardiomyocytes. Sec23 is a well-characterized marker of ER exit sites and COPII vesicles in mammalian cells [84]. In untreated cardiomyocytes, sec23 produced a pattern of immunostaining along Z-lines that was interspersed with RyR2-positive staining (Fig. 15A *and inset*). This suggested that sec23 might be bound to membrane surfaces of cisternae along Z-lines. When sec23 localization was analyzed in cells

overexpressing CSQ-DsRed, sec23 appeared to be bound to the perinuclear membrane compartment enriched in CSQ-DsRed (Fig.15B). Because CSQ-DsRed is expected to be an intralumenal ER protein whereas sec23 is a cytosolic protein, such interactions could not theoretically be direct, and would presumably require a transmembrane signal resulting from enhanced levels of lumenal CSQ-DsRed. The reason for this unexplained translocation of sec23 was not further investigated, but could reflect the inefficient ER exit of CSQ-DsRed. Sec23 levels measured by immunoblotting and densitometry exhibited a roughly 25% decrease in cells treated with Ad.CSQ-DsRed, but showed no further changes with time of adenoviral treatment (Fig. 13, rightmost panel).

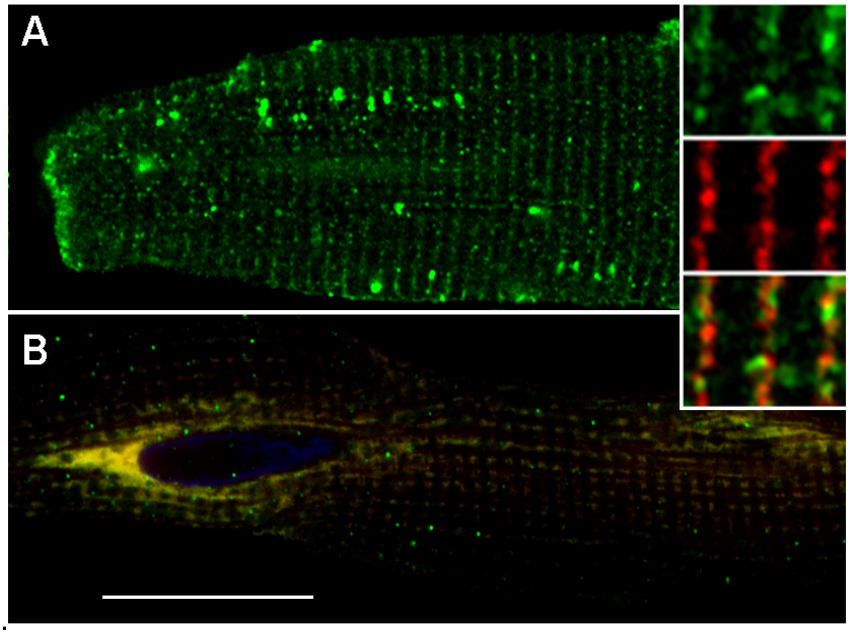

Figure 15. Sec23 subcellular localization in cultured rat cardiomyocytes. (A) cultured rat cardiomyocytes were immunostained using anti-sec23 antibodies (green), and anti-RyR2 antibodies (red, shown only in inset). Inset, sec23, RyR2, and merge (top to bottom) of representative Z-lines. (B) cultured cardiomyocytes were treated with Ad.CSQ-DsRed (red) for 48 h. Red (CSQ-DsRed) and green (sec23 immunofluorescence) channels are shown superimposed. Bar, 20 μm. Images, Leica TCS SP5.

Direct CSQ-DsRed fluorescence is distinct from indirect CSQ-DsRed immunofluorescence

Although CSQ-DsRed was readily detected on immunoblots using either anti-DsRed or anti-CSQ2 antibodies (Fig. 13), we were surprised to find that after 48 h of

DsRed overexpression, neither anti-DsRed nor anti-CSQ2 antibodies were able to detect CSQ-DsRed in the perinuclear compartments of fixed cardiomyocytes (Figs. 16-18). Instead, anti-DsRed and anti-CSQ2 antibodies prominently labeled the cell periphery. This result was seen with three separate antibodies to the CSQ-DsRed fusion protein (Fig. 17C, 17D, and 18F).

As discussed below, a likely explanation for the loss of immunoreactivity was that interaction of antibodies was lost due to the (predicted) tetrameric structure of DsRed [76-77]. This did lead, however, to a labeling of two separate pools of overexpressed CSQ-DsRed having alternate subcellular distributions. As supported in experiments

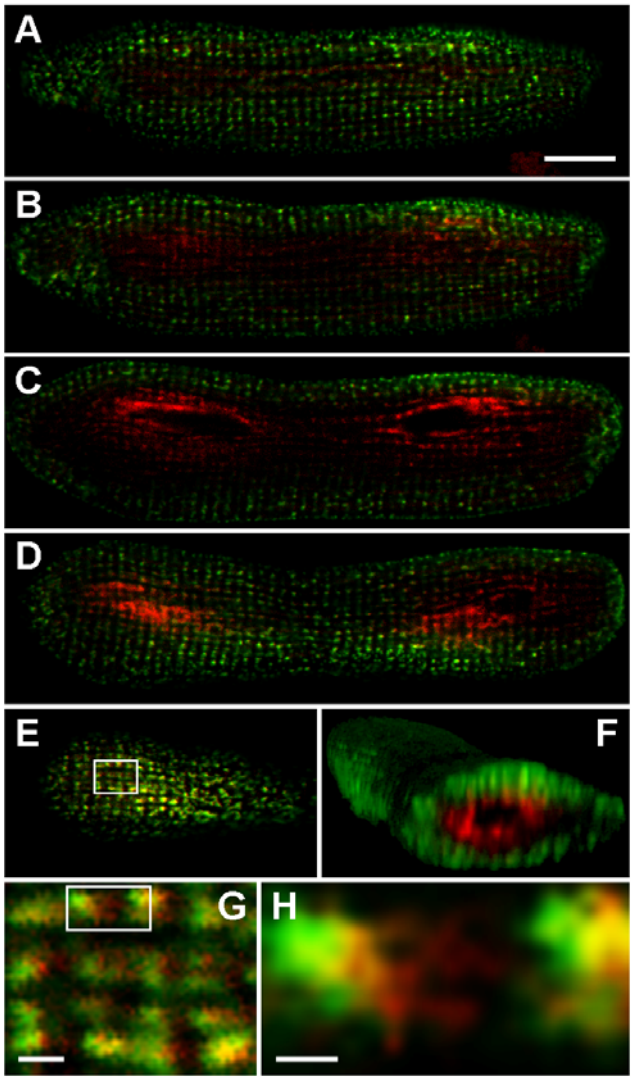

Figure 16. CSQ-DsRed fluorescence versus anti-DsRed immunofluorescence. Cardiomyocytes were treated with CSQ-DsRed adenovirus for 48 h, then fixed and stained with anti-DsRed antibodies. Confocal fluorescent images were obtained (z-stack consisting of 38 x 0.5 μm optical slices) on the Leica TCS SP5; selected slices are shown (z = 2.5, 3.5, 5.0, 8.0, 9.5 μm for panels A, B, C, D and E, respectively). CSQ-DsRed fluorescence (red) and indirect anti-DsRed (green) fluorescence are shown together in all panels (bar, 10 μm). The entire Z-stack was assembled into a three-dimensional image using the ImageJ 3D Viewer plugin in conjunction with ImageJ software, and cropped at the first nucleus in order to highlight the radial distribution and separation of CSQ-DsRed tetramers (red) and monomers (green) (panel F). An enlargement of the boxed area in E (panel G), representing a peripheral slice of the cardiomyocyte, shows the presence of CSQ-DsRed tetramer largely in compartments distinct from the monomer (bar, 1 μm). The boxed area in G was also enlarged (panel H) to show non-colocalization occurring even at the sarcomeric level, where it appears that CSQ-DsRed tetramers redirect into free-SR rete. Bar, 0.5 μm.

below, and discussed in later sections, we interpreted the red and green labeling as tetrameric CSQ-DsRed and an immunoreactive CSQ-DsRed monomer, respectively. The perinuclear versus peripheral (tetrameric versus monomeric) staining patterns were seen in sequential optical slices (z-stack), validating a 3-dimensional distribution of the direct DsRed fluorescence near the nucleus (Fig. 16A-E). Indeed, the radial nature of the direct DsRed fluorescence was apparent in virtual transverse slices of the reconstructed z-stack along its longitudinal length (Fig. 16F). Closer examination of an optical slice (panel G) near the cell periphery (panel E) where green immunofluorescence (CSQ-DsRed monomers) dominates direct red fluorescence (CSQ-DsRed tetramer), revealed an imperfect co-localization of the two forms. Higher magnification of the two fluorescent signals confirmed minor differences in distribution at the level of individual sarcomeric SR structure (panel H). Even where indirect and direct CSQ-DsRed fluorescence signals occurred together, a distinct distribution was revealed for each, perhaps suggesting that CSQ-DsRed tetramers and monomers traffic differently.

To further analyze the relationship between CSQ-DsRed fluorescence and its immunoreactive forms, we examined a time course of overexpression by confocal fluorescence microscopy. Whereas CSQ-DsRed fluorescence did not develop until about 32 h of adenovirus treatment, anti-DsRed and anti-CSQ immunofluorescence were both detected after only 16-20 h, appearing around nuclei (Figs. 17,18). Time-dependent changes in CSQ-DsRed fluorescence and immunofluorescence were consistent with its translation and accumulation in perinuclear rough ER after 16 h, followed by its increasing concentration in the same region as a red fluorescent

polymer. Once juxtanuclear polymerization occurred, CSQ-DsRed, already in junctional SR, continued its anterograde movement towards the cell periphery where it appeared to concentrate by 48 h as (green) monomer. The fact that this movement of immunofluorescent CSQ-DsRed could be visualized suggested that additional CSQ-DsRed was not being generated along the rough ER-junctional SR pathway, perhaps because all CSQ-DsRed monomer was scavenged within the perinuclear region by the polymer.

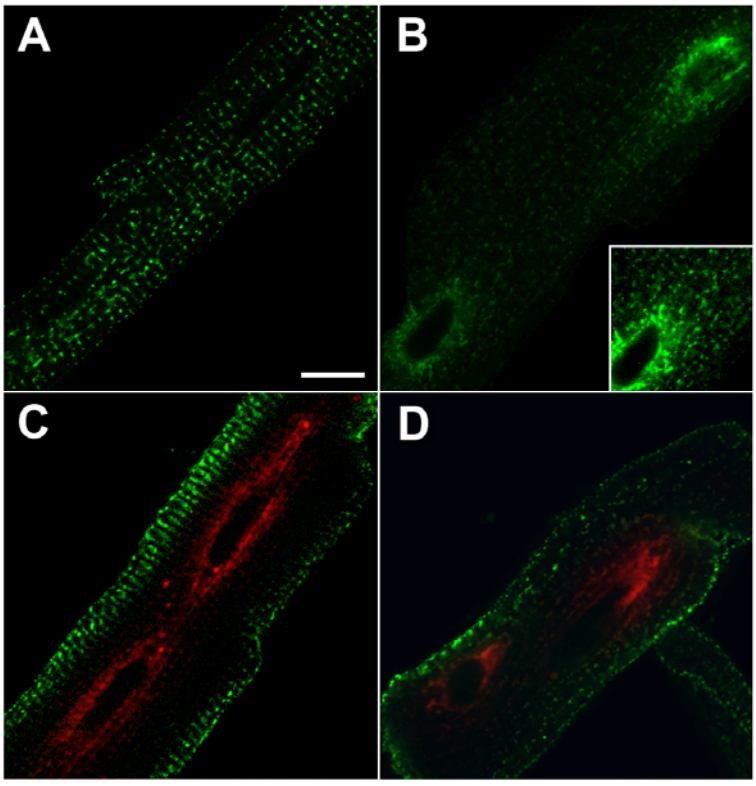

Figure 17. Time-dependent changes in anti-CSQ2 immunofluorescence during CSQ-DsRed overexpression. Cardiomyocytes were left untreated (A), or treated with CSQ-DsRed adenovirus for 20 h (B) or 48 h (C,D) before fixation and pemeabilization. Fixed cells were immunostained with monoclonal anti-CSQ2 antibodies (green) (A-C) or rabbit polyclonal anti-CSQ2 antibodies (D), and analyzed for red DsRed fluorescence and green immunofluorescence using laser confocal microscopy (Leica TCS SP5). The inset in panel B shows a portion of the cell which is brightened offline so that fluorescence of endogenous native rat CSQ2 is similar in panels A and B. Bar, 20 μm.

The fluorescence staining pattern of native rat CSQ2 could be seen in untreated (control) heart cells exhibiting a steady-state distribution characteristic of junctional SR puncta (Fig. 17A). Visualization of native rat CSQ2, however, required fluorescence acquisition times that produced overexposures of CSQ-DsRed immunofluorescence (Fig. 17B, *inset*), so was not visible with the exposure times used in subsequent figures. In contrast to the relatively unchanging pattern of native CSQ2 over a 48 h time course

(not shown), overexpressed CSQ-DsRed immunofluorescence exhibited a time-dependent trafficking.

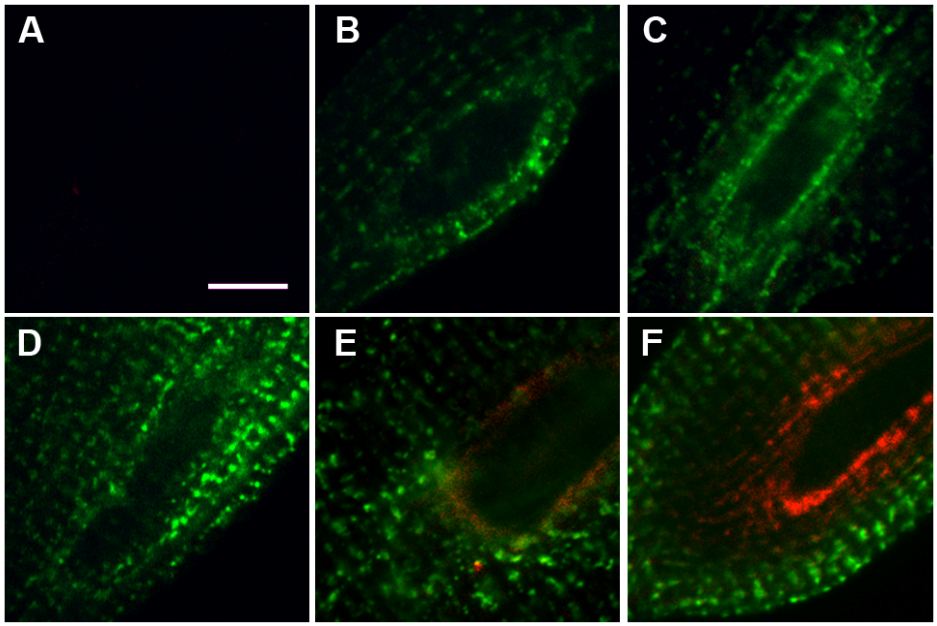

Figure 18. Time-dependent changes in CSQ-DsRed fluorescence and anti-DsRed immunofluorescence. Cardiomyocytes were left untreated (A), or treated with CSQ-DsRed adenovirus for 16 h (B), 20 h (C), 24 h (D), 36 h (E), or 48 h (F) before fixation and permeabilization. Fixed cells were immunostained with anti-DsRed antibodies (green), and analyzed for red DsRed direct fluorescence and green indirect immunofluorescence using laser confocal microscopy (Leica TCS SP5). Bar, 10 μm. Magnifications among panels are similar but may vary slightly to better illustrate structural differences.

To summarize, our data suggest that the tetrameric form of CSQ-DsRed, while necessary to produce the intense red fluorescence, was relatively incapable of interaction with antibody molecules. Meanwhile, antibodies to either half of the fusion protein detected CSQ-DsRed monomers which exhibit highly reduced, if any, intrinsic (direct) fluorescence. The data indicate that once CSQ-DsRed tetramerizes within rough ER, its anterograde trafficking is very substantially restricted, whereas molecules that do not incorporate into the polymer within the nuclear envelope, populate increasingly peripheral junctional SR sites. Based upon these new studies on CSQ2 trafficking from rough ER to junctional SR compartments, and our recent work on polymer-dependent trafficking of CSQ2 in nonmuscle cells [23, 71], we propose a new model of CSQ2 trafficking and junctional SR biology in the adult cardiomyocyte.

DISCUSSION

In nonmuscle cells, we previously concluded that CSQ2 is retained within specific secretory compartments by virtue of its polymerization [23, 71]. CSQ2 polymers accumulate in discrete secretory compartments presumably because soluble protein cargo integration into COPII vesicles is very inefficient for large polymers [71, 85-86]. In nonmuscle cells, cardiac CSQ polymers form in an early ER compartment comprised of polygonal cisternae throughout the cell, but are absent from the ERGIC [23]. This subcellular localization for CSQ2 is also reflected in the structure of its N-linked glycan, which is always found in an unprocessed form (GlcNAc2Man9,8).

Skeletal muscle CSQ localizes not to ER, but exclusively to the intermediate compartment (ERGIC) of nonmuscle cells [71]. The remarkable difference between localization of these two CSQ isoforms within the same cell type underscores the relationship between polymerization and localization in mammalian cells. Thus, not only can CSQ polymerize *in vivo*, but differences in milieu that exist within lumens of two consecutive and juxtaposed subcompartments (ER and ERGIC) are sufficient to completely discriminate and segregate these two forms of CSQ. Differences in the glycan structures on a conserved Asn^{316} in the two proteins are also consistent with the differential localization [71].

Tetramerization of DsRed is a documented aspect of its structure [76-77]; in fact, DsRed fluorescence is thought to require its tetramerization, although a monomeric form exhibiting greatly reduced fluorescence has been generated through numerous point mutations [77]. Thus, when fused with CSQ2, tetramerization of DsRed led to its effective retention, probably because of inefficient anterograde trafficking, similar to that

reported for cardiac CSQ polymers in nonmuscle cells [23, 71]. It is also possible that CSQ-DsRed tetramers led to even more complex polymers as a result of finite levels of CSQ2 polymerization that might occur even in the perinuclear region, although native CSQ2 does not typically accumulate (polymerize) in this compartment.

Anti-DsRed fluorescence and CSQ-DsRed immunofluorescence were mutually exclusive because DsRed tetramerization simultaneously produces a bright red fluorescence [77] while effectively turning off antibody detection. This generated separate assays for polymeric versus monomeric protein molecules that exhibited distinct patterns of intracellular trafficking. Time-dependent features of the overexpression of CSQ-DsRed were particularly revealing. CSQ-DsRed was initially detectable only by immunoreactivity, where it had a juxtanuclear localization. At longer times, immunoreactive perinuclear CSQ-DsRed was replaced with the bright red fluorescence expected for DsRed tetramers in the same compartment. However, whereas immunoreactive (monomeric) CSQ2 trafficked out of the perinuclear region, albeit slowly (Figs. 17,18), the red fluorescent tetramer was too large to traffic to junctional SR puncta to any significant extent [71, 85-86].

By the end of a 48 h incubation period, the entire immunoreactive pool of CSQ2 was concentrated at the cell periphery (Fig. 16F). If immunoreactive CSQ-DsRed represents monomeric CSQ-DsRed, then the shift of this pool of protein from the perinuclear region to the cell periphery suggests that the input of additional immunoreactive CSQ-DsRed protein molecules was no longer occurring. This may be directly due to the scavenging of all newly synthesized CSQ-DsRed within the fluorescent polymer within the perinuclear region once formed. Thus, without further

input of newly-synthesized CSQ-DsRed, the "pulse" of monomeric CSQ-DsRed that escaped juxtanuclear polymerization could be visualized as it moved through the full extent of the Z-line localized ER/SR pathway. The fate of this CSQ-DsRed that concentrated in the cell periphery after 48 h was not investigated in this study, but represents an interesting question for future studies.

Protein markers of the ER translocon complex, TRAPα and TRAM, also had a juxtanuclear localization in the cardiomyocyte, suggesting that this is a major site of rough ER and CSQ2 biosynthesis. Rough ER was previously visualized by electron microscopy in a continuum with the nuclear membrane, as one of a few morphologically-defined sites within adult rabbit cardiomyocytes [87]. Translation around myonuclei in cardiomyocytes for specific cardiac proteins has not been reported to our knowledge, but has been discussed as one of at least two such sites in skeletal muscle myocytes [88].

CSQ-DsRed fluorescence could be observed connecting the perinuclear region directly to adjacent junctional SR (RyR2-positive) puncta in optical sections that bisected the myonuclear midline (Figs. 12E, 14B2, *asterisk*). A pathway for SR membrane protein trafficking along Z-lines has not previously been reported in cardiomyocytes, but may be similar to the exporting ER network described by Kaisto and Metsikkö in rat skeletal muscle myofibers [89]. We also observed apparent longitudinal trafficking of CSQ-DsRed, particularly when CSQ-DsRed-containing cisternae were viewed near the outer edges of the cell (Fig.16E,G,H). A mechanism of longitudinal trafficking of CSQ2 is also not known, but our data for sec23, a microtubule-based trafficking protein of COPII vesicles [84], suggests that junctional SR to

longitudinal SR might represent the normal direction of protein trafficking in the cardiac secretory pathway. Free SR is enriched in proteins that contain the C-terminal KDEL retrieval sequence [90-92]. Because KDEL proteins are thought to be enriched in both ER and ERGIC [23, 93], their presence is consistent with free SR being a subcellular compartment distal to junctional SR. The view of junctional SR as equivalent to ER, and longitudinal (or free) SR as being equivalent to the intermediate (ERGIC) compartment is consistent with studies from the Metsikkö laboratory in skeletal muscle myofibers [89, 94]. Similar to the limited accumulation of CSQ-DsRed in longitudinal SR (Fig. 16H), native CSQ2 that escapes retention by polymerization should also traverse this part of the cardiac secretory pathway, as do the other muscle-specific luminal ER/SR Ca^{2+}-binding proteins sarcalumenin and histidine-rich Ca^{2+}-binding protein [17].
In a new model of CSQ2 biosynthesis and trafficking in cardiomyocytes (Fig. 19), we propose that CSQ2 is synthesized at sites within the nuclear envelope, and then traffics directly to junctional SR in the direction of the cell surface. In the case of CSQ-DsRed, polymers (tetramers) are retained in rough ER and traffic slowly towards distal junctional SR only as tetramers dissociate to monomers. We infer from these data that CSQ2 normally polymerizes only within junctional SR puncta, a process that prevents or slows its anterograde trafficking, and presumably its secretion. We conclude therefore, that, as in the case of mammalian nonmuscle cells, CSQ2 polymerizes in junctional SR because it is the first intracellular compartment that satisfies the biophysical criteria for polymerization.

The model presented here may help to explain previously reported CSQ2 protein structures in normal and hypertrophied hearts from small dogs [35]. In beagle heart

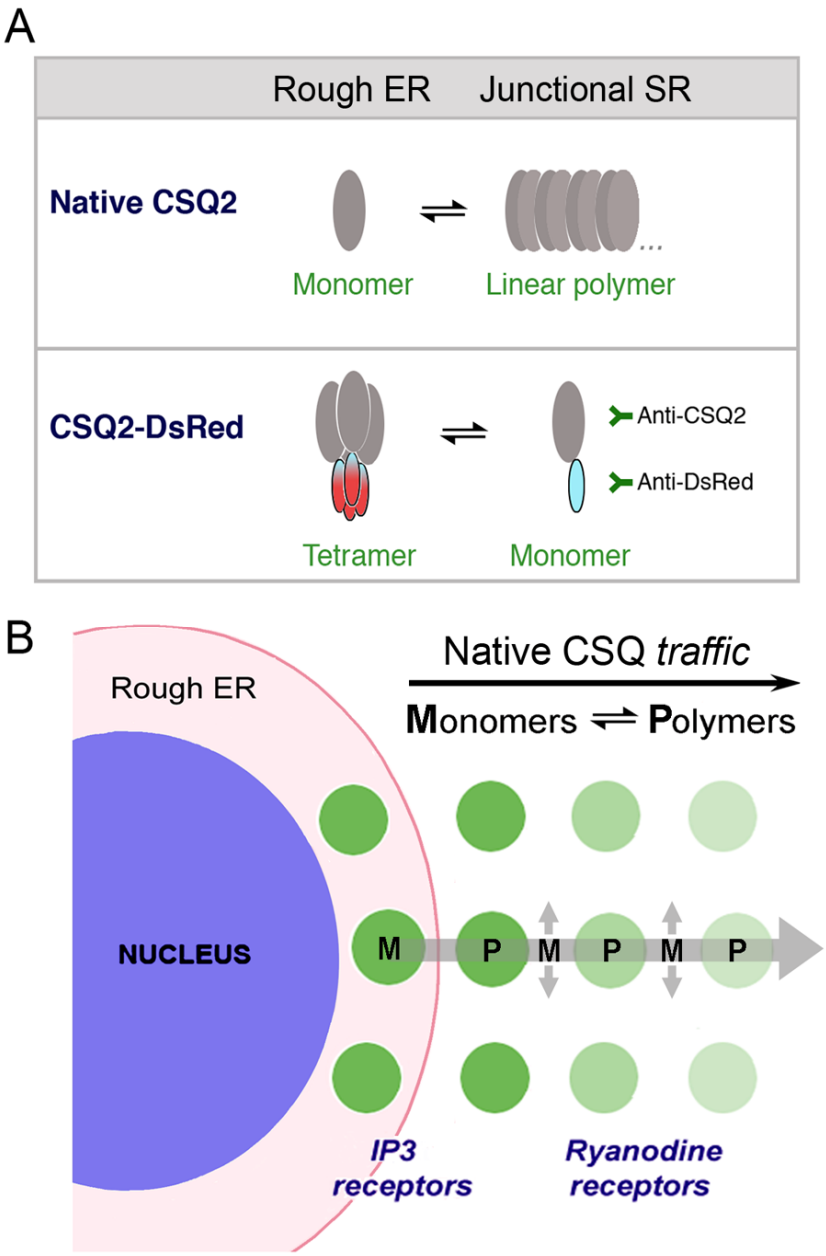

Figure 19. Model of native CSQ2 trafficking from rough ER to junctional SR in cardiomyocytes. (A) Native CSQ2 exists as monomers or linear polymers in dynamic equilibrium inside the secretory pathway of cardiomyocytes. While monomeric CSQ2 traffics anterogradely, polymeric CSQ2 cannot, leading to its accumulation in junctional SR puncta. CSQ-DsRed, in contrast to native CSQ2, polymerizes and accumulates in rough ER around nuclei. CSQ-DsRed monomers, like CSQ2 monomers, can traffic anterogradely where they can be specifically detected by antibodies against either half of the fusion protein pair. Not shown in this scheme are forms of CSQ2 in junctional SR that might contain CSQ-DsRed linear homopolymers and heteropolymers (with native CSQ2). (B) In cardiomyocytes, native CSQ2 is synthesized in perinuclear rough ER. Trafficking proceeds across a direct cellular transport pathway (large arrow) to perinuclear junctional SR, dependent on a dynamic polymer (P)-monomer (M) equilibrium. A predominance of native CSQ2 monomers in rough ER and along the rough ER-junctional SR trafficking pathway led to anterograde trafficking. CSQ2 polymers form within junctional SR puncta due to its distinctive intraluminal ionic conditions, leading to its accumulation [71]. ER-exit sites along this same ER pathway (highlighted by sec23 immunostaining, cf. Fig. 15), may separate the basic cardiac ER (junctional SR) from an intermediate compartment (longitudinal SR) that traffics along myofibrils (smaller arrows). In the case of CSQ-DsRed overexpression in cardiomyocytes, tetrameric CSQ-DsRed accumulates in rough ER. Protein monomers of CSQ-DsRed predominantly traffic anterogradely to accumulate in peripheral junctional SR puncta. Puncta in close proximity to cardiomyocyte nuclei may contain the inositol trisphosphate (IP3) receptor in addition to, or instead of the more prominent ryanodine receptor contained in more peripheral junctional SR puncta [95].

tissue, CSQ2 molecules can be divided into two types based upon their glycan structures. Most CSQ2 glycans show extensive mannose trimming (Man3-5), indicative of junctional SR localization [31, 34], but a minor portion of CSQ2 contains glycans indicative of rough ER localization (Man8,9) [23, 31]. This rough ER portion of CSQ2 doubles in rapid-pacing induced heart failure, as does its state of phosphorylation [35]. Moreover, ER forms of CSQ2 (Man9,8) in heart are fully phosphorylated, whereas junctional SR forms of CSQ2 (Man 3-6) are increasingly dephosphorylated [34]. Phosphorylation by protein kinase CK2 may thus be responsible for its rough ER retention.

CONCLUSIONS

In summary, CSQ-DsRed fluorescence and immunofluorescence reveal several new aspects of CSQ biology by essentially slowing down its secretion, and by causing it to polymerize in a proximal compartment (rough ER). Our new findings and accompanying model include: 1) the identification of the subcellular site of CSQ2 biosynthesis (cardiac rough ER), 2) demonstration of a CSQ2 polymerization-dependent compartmentalization in cardiomyocytes, 3) the suggestion that CSQ-DsRed traffics directly from rough ER to junctional SR along a novel, albeit uncharacterized intracellular pathway, and 4) the characterization of rough ER and junctional SR as cardiac ER, and longitudinal SR as a compartment distal to ER exit sites possibly corresponding to ERGIC. These data and model may aid in understanding the changes in CSQ2 and SR biology associated with new transgenic models and in diseases associated with inner membrane biology in adult cardiomyocytes.

CHAPTER 3

IDENTIFICATION OF CARDIAC CALSEQUESTRIN KINASE AND THE EFFECTS OF C-TERMINAL PHOSPHORYLATION

ABSTRACT

The luminal SR protein CSQ2 contains phosphate on roughly half of the serines found in its short cardiac-specific C-terminus. The sequence around the phosphorylation sites in CSQ2 suggest that the *in vivo* CSQ2 kinase is protein kinase CK2, even though this enzyme is thought to be present only in the cytoplasm and nucleus. To test whether CSQ2 kinase is protein kinase CK2, we combined experimental approaches directed at reducing the effects of CSQ2 phosphorylation in intact cells. *In vitro,* tetrabromocinnamic acid (TBCA, 100 μM) inhibited both CSQ2 kinase and CK2 activities by about 85% over the same range of concentrations. In intact cultured primary adult rat cardiomyocytes and in COS cells, 24 h of TBCA (100 μM) treatment produced a roughly 75% decrease in phosphorylation of CSQ2. To further validate the identity of CSQ2 kinase as protein kinase CK2, we down-regulated both CK2α subunits in COS cells by transfection of appropriate siRNA, producing an 85-90% decrease in CK2α and CK2α′ protein levels. CK2-silenced cells exhibited a two-fold reduction in CSQ2 kinase activity. Endogenous CSQ2 overexpressed in CK2-silenced COS cells was also reduced by a factor of two. These pharmacologic and biochemical data suggest that CSQ2 in intact cells is phosphorylated by CK2, a cytosolic kinase (CK2) that could phosphorylate CSQ2 only during or before nascent protein translocation. When CSQ2 phosphorylation site mutants were analyzed in COS cells, the characteristic rough ER form of the CSQ2 glycan (GlcNAc2Man9,8)

underwent phosphorylation-site dependent processing such that CSQ2-nonPP (Ser to Ala mutant) and CSQ2-mimPP (Ser to Glu mutant) produced apparent lower and greater levels of ER retention, respectively. Taken together, our data support a hypothesis in which CK2 is able to phosphorylate CSQ2 co-translationally at biosynthetic sites in rough ER, a process that results in changes in its subsequent movements through the secretory pathway.

INTRODUCTION

Calsequestrin is a resident luminal protein of the SR [11, 19-20, 22, 33, 96] where an involvement in junctional Ca^{2+} release is assumed to be its primary function [13, 30]. The fast-twitch skeletal muscle CSQ1 and cardiac CSQ2 isoforms come from independent genes but share a relatively conserved sequence [33, 97]. Mammalian CSQ2 proteins have an 18-25 residue C-terminal extension that contains multiple serines in an otherwise highly acidic sequence, and is not present in CSQ1 [33, 98]. These C-terminal serines are prolific *in vitro* substrates for an endogenous protein kinase, making CSQ2 by far the most heavily phosphorylated protein in heart cell homogenates, in the absence of exogenous kinase activators such as cyclic AMP [34]. It is similarly phosphorylated in all mammalian cells following its overexpression [23, 31, 34].

Both CSQ2 phosphorylation state and Asn(N)-linked glycan structure can be simultaneously determined by mass spectrometric analysis of purified CSQ2 protein [31, 35]. From these analyses, a great deal of information about the relationship between CSQ2 phosphorylation and its trafficking has been obtained. For example, pathways of CSQ2 trafficking are revealed in the CSQ2 glycan structures, and it

appears clear that no CSQ2 in heart or nonmuscle cells ever leaves ER compartments. The CSQ2 glycan is comprised of only high-mannose structures GlcNA2Man*N,* where *N* = 3-9 depending upon the extent of mannose trimming [31, 34-35]. Recently, we have described novel ER-to-SR intracellular trafficking pathways in the adult cardiomyocyte, concluding that junctional SR represents bona fide ER. CSQ2 traffics directly from juxtanuclear rough ER to junctional SR where it is retained by its polymerization [99]. Mannose trimming accompanies its anterograde trafficking in nonmuscle cells, whereas it is a hallmark of its rough ER to junctional SR trafficking in cardiac myocytes [23, 31, 34]. We have also hypothesized that the longitudinal SR corresponds to the intermediate compartment (ERGIC), requiring proteins such as SERCA2a to enter ER exit sites that lie along the junctional SR pathway [99].

Mass spectrometry of intact purified CSQ2 also reveals significant insights into its phosphorylation. When analyzed from heart tissue, newly synthesized molecules (having unprocessed glycans (Man9,8)) are found to exist only in the completely phosphorylated state [34]. Conversely, as CSQ2 undergoes mannose trimming in its trafficking to junctional SR, the number of unphosphorylated molecules dramatically increases, such that the most highly trimmed glycans contain no phosphate [34]. When analyzed in cultured nonmuscle cells, it is also evident that anterograde trafficking is also accompanied by CSQ2 dephosphorylation [23, 31, 34].

Despite considerable knowledge about the CSQ2 phosphorylation reaction in nonmuscle cells and cardiac myocytes, the identity of the CSQ2 kinase has not yet been established. There are no known luminal serine/threonine kinases identified in the literature, to our knowledge, that could serve as a candidate CSQ2 kinase *in vivo.* The

putative identity of CSQ2 kinase derives from the fact that its C-terminal phosphorylation sites (Table 2) matches closely a consensus sequence (S/T-X-X-D/E) for the cytosolic serine/threonine protein kinase CK2 (formerly casein kinase 2) [37-38]. CSQ2 is also a very efficient *in vitro* substrate for CK2 [34, 36].

A paradox, however, results if one assumes that CK2 is the CSQ2 kinase, as CK2 has no signal sequence for gaining access to the ER lumen [100], whereas CSQ2 is thought to be wholly contained within the SR lumen throughout its lifetime [12, 33]. One hypothetical mechanism for reconciling the lack of co-localization with a co-translational phosphorylation event would be that CSQ2 phosphorylation occurs prior to nascent polypeptide translocation across the rough ER membrane [64].

Mammalian protein kinase CK2, in the holoenzyme form, is composed of two separate catalytic subunits and two identical regulatory subunits [101]. The catalytic subunits, CK2α and CK2α′, share approximately 90% homology and are the product of different genes [44, 102-103]. Both catalytic subunits are capable of phosphorylating substrates independent of holoenzyme formation, and have been localized to different areas of the cell [101, 104-105]. CK2 has been shown to promote cell proliferation [106], and has recently become a chemotherapeutic target in order to promote tumor regression [107] leading to the advent of a series of new and highly specific inhibitors [61].

In this study, we have combined cellular and molecular approaches to investigate the actions of protein kinase CK2 on the cardiac-specific C-terminus of CSQ2. Reduced CSQ2 phosphorylation produced by reversible CK2-specific inhibitors, loss of CK2 protein by siRNA, and loss of phosphorylation by sequence mutations all support a

hypothesis in which phosphorylation of CSQ2 by the cytosolic protein kinase CK2 occurs co-translocationally in rough ER to affect subsequent anterograde trafficking.

MATERIALS AND METHODS

Antibodies and commercial proteins

Monoclonal antibody specific to CSQ2 was the generous gift of Dr. Larry Jones, Indiana University School of Medicine. Mouse monoclonal antibody raised to human protein kinase CK2α catalytic subunit (CSNK2A1) and rabbit polyclonal antibody raised to human protein kinase CK2α′ catalytic subunit (CSNK2A2) were purchased from Abcam (ab70774 and ab10474). Human CSNK2A1 (His-tagged CK2α) and CSNK2A2 (GST-tagged CK2α′) recombinant proteins were purchased from Invitrogen (PV3248 and PV3624).

Cell culture

COS-7 African green monkey kidney (COS) and human embryonic kidney 293 cells (HEK-293), purchased from American Type Culture Collection, were cultured in Dulbecco's Modified Eagle's Medium (DMEM) containing 25 mM HEPES, pH 7.4, 10% fetal bovine serum, 100 units/ml penicillin G, 0.1 mg/ml streptomycin and 0.25 μg/ml amphotericin B, at 37 °C with 5% CO_2.

Cardiomyocyte preparation

Rat ventricular cells were enzymatically dissociated using a Langendorff perfusion apparatus, as previously described [99]. Heart cells were cultured on laminin-coated dishes in modified Medium 199 containing 2% bovine serum. Protein concentrations were determined according to Lowry *et al*. [108].

CSQ2 plasmid and adenoviral constructs

CSQ2 constructs and viral inserts were generated from wild type canine cardiac CSQ2 cDNA [33]. Creation and purification of adenoviruses for wild-type CSQ2 (Ad.CSQ) and the non-phosphorylatable mutant Ad.nonPP (Ser 378,382,386 Ala) were previously described [31]. The phosphorylation mimic CSQ2 mutant Ad.mimPP was produced in an identical manner to that of Ad.nonPP except glutamates were used to replace the C-terminal serines (Ser 378,382,386 Glu). Briefly, the mutating reverse primer (67-mer) contained 3 single base changes necessary for the Ser to Glu conversion. PCR products were cloned into pBluescript (Stratagene), sequenced by the dideoxy method [109], and then subcloned into the pShuttle plasmid for virus construction (AdEasy System, American Type Culture Collection).

Adenovirus-mediated overexpression

Cells were treated with recombinant adenoviruses at a multiplicity of infection (MOI, pfu/cell) of 50 or 100 for COS and heart cells [31]. Purified viruses were added to cultured cells at the time of plating and left on throughout the overexpression period.

Purification of overexpressed CSQ2

Purification of CSQ2 from COS and cardiomyocyte cultures was carried out two days post-infection, as previously described [31] but with minor modifications. Cell pellets were resuspended at roughly 1 mg/ml in extraction buffer containing 10 mM Tris, pH 8.0, 250 mM NaCl, 1% Triton X-100 and 1 mM EGTA. Extracts were centrifuged at 25,000 x g for 30 min, bound to 40 µl DEAE-Sephacel (Amersham Biosciences), washed, then eluted with 100 µl extraction buffer containing 500 mM NaCl. SDS-PAGE analysis was carried out according to Laemmli [74].

Preparation of native CSQ2 kinase sources

Freshly isolated adult rat cardiomyocytes and cultured COS cells were pelleted and washed in PBS. The pellets were resuspended in low ionic strength media containing 5 mM MOPS, pH 8.0, 1 mM EGTA and protease inhibition cocktail (Sigma P8340). Suspensions were incubated on ice for 10 min and then passed through a $25^{5/8}$ ga. needle and glass/teflon homogenizer 10 times each. NaCl was added to the resulting lysates (homogenates) to a concentration of 100 mM. Detergent mixtures were created by adding Triton X-100 to the homogenates to a final concentration of 1%. Identical volumes (0.5 ml) of homogenates, detergent-free and detergent extraction mixtures were subjected to high speed centrifugation (30,000 x g_{max} for 15 min) in order to obtain homogenates and extracts.

In vitro phosphorylation of purified CSQ2

The standard CSQ2 phosphorylation reaction mixture for "back phosphorylation" consisted of 20 mM MOPS, pH 8.0, 150 mM NaCl, 0.5 mM EGTA, 10 mM $MgCl_2$, and contained 20 μM [γ -^{32}P]ATP (3000 cpm/pmol), 2 μg purified CSQ2 substrate, and a source of CSQ2 kinase, brought to a total volume of 50 μl with distilled water. As a CSQ2 kinase source, either 2 μg of COS cell or cardiomyocyte homogenate or detergent extract was used, as indicated; or 0.1-0.4 μg purified human CK2α or CK2α' kinase was added as indicated. Quantification of phosphate incorporation was determined by SDS-PAGE, autoradiography, and scintillation counting of radioactive bands excised from dried gels. Measurements of "front phosphorylation", or endogenous phosphorylation, included a pretreatment with or without 0.01 U acid phosphatase (P0157, Sigma) for 60 min in 10 μl of 30 mM MES buffer, pH 5.8, 0.1 mM

EGTA, as previously described [36], then dilution into phosphorylation buffer to a final volume of 50 *µ*l. For comparison with CK2α' commercial protein kinase activities, 2 µg of CSQ2 was used as substrate and equal units of kinase were compared: CK2α was 0.5 U/µg, CK2α' was 0.25 U/µg (1 U = nmol P_i /mol RRRDDDSDDD peptide/min).

Inhibition of CSQ2 kinase using specific inhibitors of protein kinase CK2

The CK2 specific inhibitors tetrabromocinnamic acid (TBCA, Calbiochem), 2-dimethylamino-4,5,6,7-tetrabromo-1H-benzimidazole (DMAT, Calbiochem) and 4,5,6,7-tetrabromobenzotriazole (TBB, Sigma) were dissolved in DMSO then diluted into phosphorylation reactions to varying micromolar concentrations to establish which was the most potent and gave the most consistent results. To inhibit CSQ2 phosphorylation in intact cells, COS or heart cells were plated in 6-well dishes with Ad.CSQ for 24 h. TBCA (100 µM) or DMSO was then added for a total incubation time of 48 h, then cells were harvested for analysis.

Mass spectrometry

For mass spectrometry of CSQ-WT, CSQ-nonPP, and CSQ-mimPP, recombinant proteins were produced in HEK cells following the addition of respective viruses. CSQ2 was purified and prepared for electrospray ionization mass spectrometry as previously described [23].

RNAi

HEK and COS cells were grown in 100 mm culture dishes for 24 hrs with or without Ad.CSQ or Ad.nPP, then transfected using DharmaFECT 1 transfection Reagent (Thermo Scientific T-2001-01), for 48 h with 100 nM Dicer-Substrate RNAi (DsiRNA, IDT), designed to silence either CSNK2A1 (IDT #HSC.RNAI.N177559.10.3),

CSNK2A2 (IDT #HSC.RNAI.N001896.10.2), or a combination of both. Negative controls included no siRNA or DS NC1 universal DsiRNA negative control (IDT). Detergent extracts were created for use with standard back and front phosphorylation assays described above, after normalization by protein assay.

mRNA analysis

RNA extraction from COS cells overexpressing Ad.CSQ was performed using RNeasy Fibrous Tissue Mini Kit (Qiagen) according to manufacturer's protocol. RNA concentrations were determined by spectrophotometer at 260 nm. One microgram of DNase-treated total RNA was reverse transcribed using a high-capacity cDNA reverse transcription kit (Applied Biosystems). Quantitative real-time PCR (qPCR) with fast SYBR green (Applied Biosystems Step One with v2.0 software) was performed using CSQ2 primers designed to span one intron. Relative quantitation was then used to evaluate mRNA levels compared to GAPDH internal control. Canine CSQ2 forward primer: 5′- CCA AGC TTG CCA AGA AGC TGG GT -3′, reverse primer: 5′- ACG TCA GCT GCA AAC TCG CCA -3′.

RESULTS

Optimization of CSQ2 phosphorylation assays

Native and overexpressed canine CSQ2 is phosphorylated in heart or nonmuscle cells on the same sites, and the reactions are assumed to occur by a similar CSQ2 kinase associated in some way with the ER [31, 34]. We analyzed CSQ2 kinase activity from both primary rat cardiomyocytes and COS cells. Both cell types were homogenized in the presence of Triton X-100 detergent to make CSQ2 kinase available to phosphorylate purified canine CSQ2 *in vitro*. Determinations of reaction linearity as a

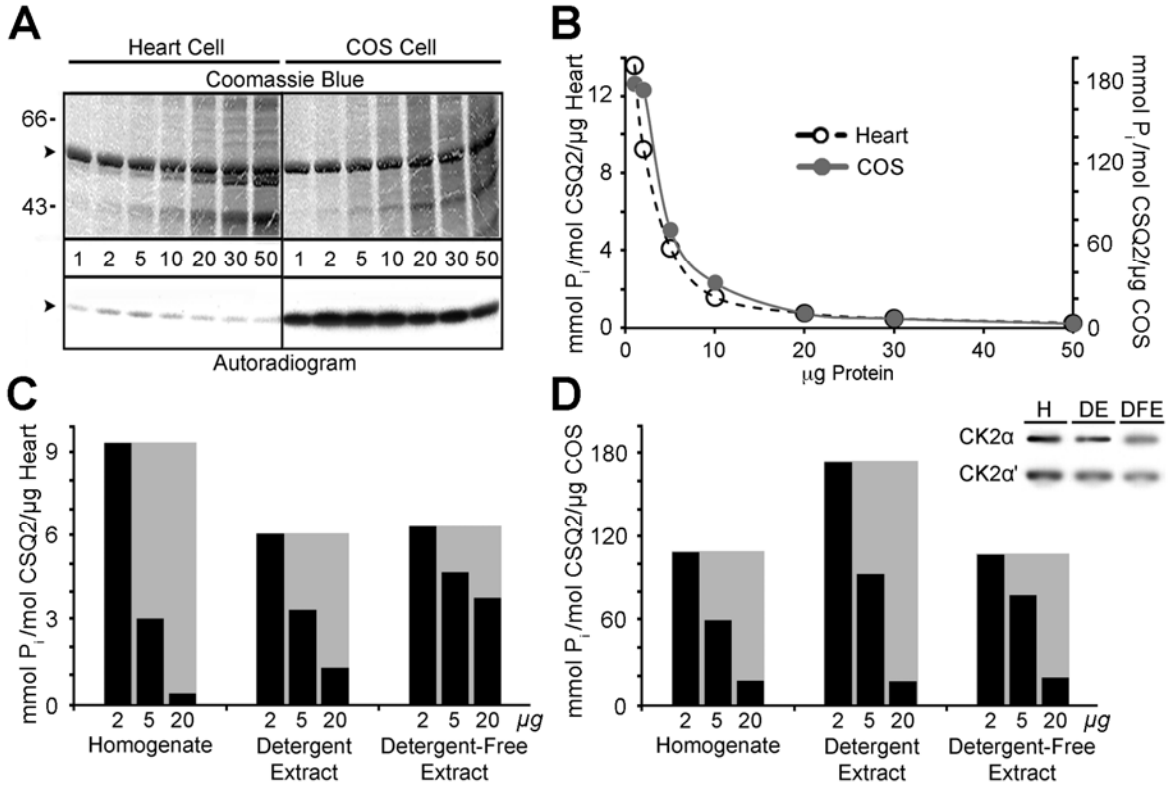

Figure 20. Effects of cellular protein on CSQ2 kinase activity. (A) increasing concentrations, 1, 2, 5, 10, 20, 30 or 50 µg of rat heart cell detergent extract or COS cell homogenate was used to phosphorylate 2 µg of purified native canine CSQ2 (*arrowheads*). Reaction mixtures were analyzed by SDS-PAGE (*MW markers, 66 and 43 kDa*) and [^{32}P]autoradiography. (B) radioactive incorporation was determined, and kinase activity is shown on the y-axis. (C,D) CSQ2 kinase activity was measured in 2, 5 or 20 µg of homogenate, from a mild-detergent extraction of 2, 5 or 20 µg of homogenate, or from a detergent-free extraction of 2, 5 or 20 µg of homogenate derived from cardiomyocytes (C) or COS cells (D). *Inset*, immunoblot of CK2α or CK2α' subunits from 50 µg of COS cell homogenate (*H*), detergent extract (*DE*), or detergent-free extract (*DFE*).

function of protein (kinase source) were carried out with varying amounts of homogenate protein. In contrast to an expected linear relationship between protein and kinase activity, increasing protein concentration actually exhibited an inverse relationship with CSQ2 phosphorylation (Fig. 20A,B); that is, increasing homogenate protein produced decreasing levels of [^{32}P]-phosphate incorporation. To remedy this extreme nonlinearity, we tested whether linearity could be better achieved using either a mild detergent extract or non-detergent extraction to separate the CSQ2 kinase from

possible interfering phosphatases or ATPases that might account for this effect. We found that linearity was partially restored with extractions carried out in detergent, and more fully restored if detergents were removed (Fig. 20C,D). Whether restoration of linearity was due to removal of CSQ2 phosphatase or cellular ATPases was not further investigated. Based upon these determinations, CSQ2 kinase activities were generally measured using 2 µg of mild detergent extract. Although the efficiency of CSQ2 kinase extraction could not be determined in these experiments because of the non-linearity, protein kinase CK2 recovery was only about 50% in detergent-free extracts based upon immunoblot analyses (Fig. 20D, *inset*).

Pharmacological inhibition of CSQ2 phosphorylation in vitro

Because of our previous *in vitro* evidence implicating CK2 as CSQ2 kinase [36], we tested the effects of new commercially available competitive inhibitors of CK2 [63] on CSQ2 kinase activity in cell extracts. To allow us to compare effects of CK2-specific inhibitors, we first normalized endogenous CSQ2 kinase activities in myocytes, COS cells, and commercial CK2 by comparing their relative ability to phosphorylate 2 µg pure CSQ2. Based upon these determinations, one would calculate that about 0.07% of cardiomyocyte protein and 1.7% of COS cell protein is CK2, if CK2 and CSQ2 kinase are the same protein and purified CK2α' maintains its native activity. A value based upon immunoblotting of pure CK2 and COS cell extracts was closer to 1% of total protein, and consistent with a 25-fold lower level in cardiomyocytes (data not shown).

Equal CSQ2 kinase activities from all three sources were then used to test inhibitors *in vitro*, using 2, 5, 10, 20, 50 or 100 µM concentrations of CK2-specific inhibitors TBB [110], DMAT [111] and TBCA [60] (Fig. 21A-C). All three inhibitors were

capable of inhibiting endogenous CSQ2 kinase activity in both cardiomyocyte and COS cell extracts, and at concentrations similar to those required to inhibit commercial CK2 phosphorylation of CSQ2. The most potent of the three inhibitors was TBCA, which

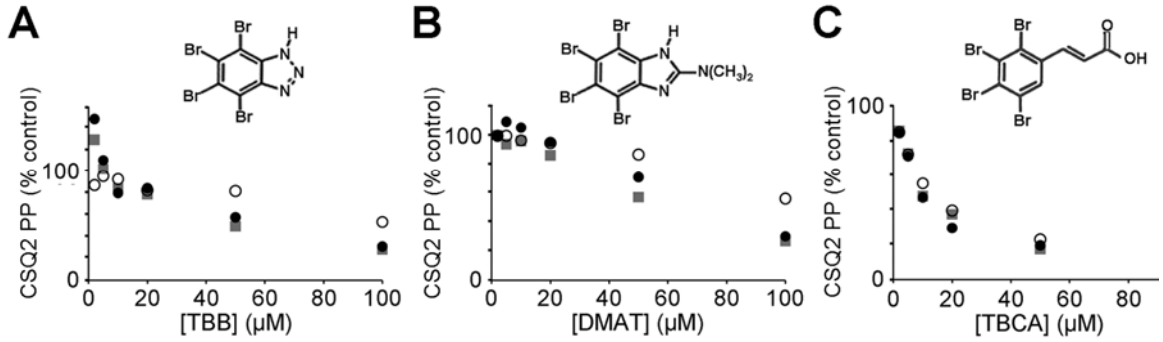

Figure 21. Effects of CK2 inhibition on CSQ2 kinase activity. Measurements of CSQ2 kinase activities were carried out as described in Experimental Procedures using equivalent amounts of activity from cardiomyocytes (*closed circles*), COS cells (*closed squares*), or pure CK2α' (*open circles*). Reactions included 0, 2, 5, 10, 20, 50 and 100 μM concentrations of the CK2 inhibitors TBB (A), DMAT (B) or TBCA (C) (structures shown in respective insets). Activities are shown (*y-axis*) as percent of control (untreated).

inhibited both endogenous CSQ2 kinase as well as commercial CK2 phosphorylation of CSQ2 at an IC_{50} of about 10 μM. TBCA produced a near identical inhibition curve for all three kinase source reactions (Fig. 21C). TBB and DMAT were also capable of inhibiting CSQ2 kinase and commercial CK2, but at higher micromolar concentrations (IC_{50} approximately 50 and 60 μM, respectively). TBCA was chosen for subsequent experiments in cultured cells because it is reportedly the most specific and potent inhibitor of the three [60], and because we found TBCA to be the most soluble in culture media (data not shown).

Pharmacological inhibition of CSQ2 phosphorylation in cultured cells

Our ability to inhibit cardiomyocyte and COS cell CSQ2 kinase *in vitro*, led us to determine whether TBCA would inhibit phosphorylation of CSQ2 during its overexpression in COS cells. For both cell types, CSQ2 was overexpressed using an

adenovirus to achieve high levels of biosynthesis in case CSQ2 phosphorylation was tied to its rate of translation. We previously showed using $^{32}P_i$-labeling in rat cardiomyocytes that endogenous CSQ2 phosphorylation is very low compared to similar amounts of virally overexpressed CSQ2 [34]. In experiments here, cardiomyocytes and COS cells were treated with Ad.CSQ for 24 h before an additional treatment with either 100 μM TBCA or vehicle (DMSO). Levels of endogenous phosphate on CSQ2 were determined from the difference between CSQ2 phosphorylation with and without phosphatase pretreatment. We found that TBCA produced a potent inhibition of phosphate incorporation into CSQ2 in cultured cardiomyocytes and COS cells of 82 and 66%, respectively, compared to vehicle controls (Fig. 22). The reduced effect of TBCA on CSQ2 phosphorylation in COS cells might just reflect the high levels of kinase in COS cells (Fig. 20B).

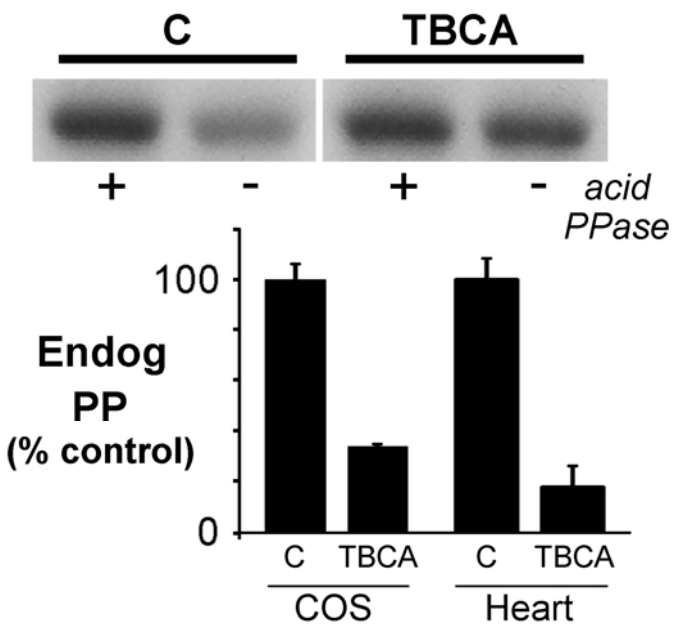

Figure 22. Reduction in endogenous CSQ2 phosphorylation in cells treated with TBCA. COS cells or cardiomyocytes (*Heart*) were treated with Ad.CSQ for 24 h in culture, then DMSO (*C*) or 100 μM TBCA was added for 24 h. Cells were extracted in mild-detergent, and levels of phosphate on the overexpressed CSQ2 (*Endog PP*) were determined for equal volumes of C or TBCA-treated cell extracts using the front phosphorylation assay. Endogenous phosphate on CSQ2 corresponds to the difference in radioactivity between ^{32}P-incorporation after and before acid phosphatase (*PPase*) treatment. A sample autoradiogram is shown for a measurement on partially purified CSQ2 protein from COS cells (*upper panel*). Results are also shown for multiple analyses of endogenous CSQ2-phosphate content following its overexpression in either COS cells or cardiomyocytes for C or TBCA-treated cells (*lower panel*, means ± S.E.M., n=3).

siRNA knockdown of CK2 catalytic subunits

To corroborate the pharmacologic data that supported identification of CSQ2 kinase as CK2, RNAi experiments were performed. Three separate siRNA mixtures that were tested were successful in silencing CK2α and CK2α' catalytic subunits at 100 nM in either HEK or COS cells, as determined by immunoblotting of cell homogenates (Fig. 23A). CK2α and CK2α' siRNA with the greatest knockdown efficiencies were used

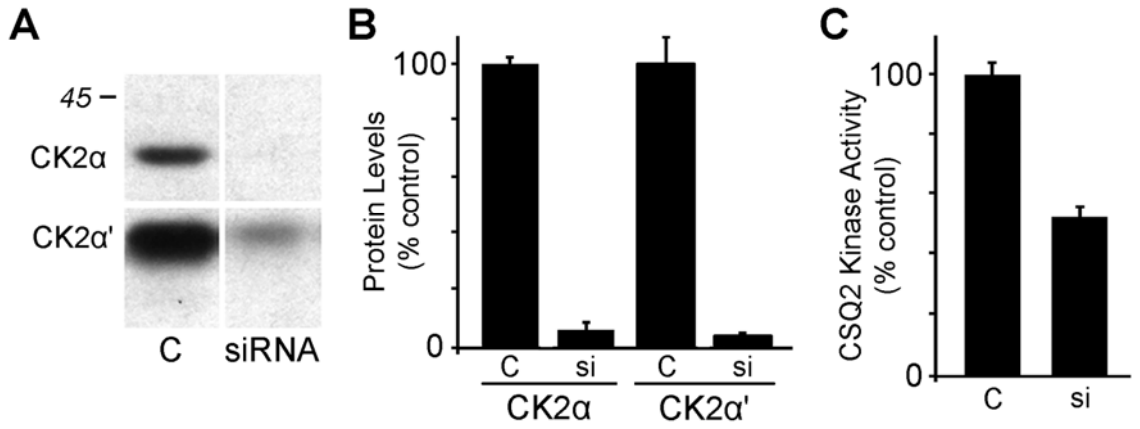

Figure 23. Knockdown of CK2α and CK2α' using siRNA. COS cells were transfected for 48 h with siRNA against either CK2α or CK2α', then extracted in mild detergent. (A) untreated cells ("*C"*) or siRNA-treated cell samples (50 µg) were analyzed by immunoblotting using specific antibodies to detect CK2α (~40 kDa) or CK2α' (~35 kDa); compare to 45 kDa MW standard. (B) shows the average levels of CK2α and CK2α' knockdown (*si*) as a percent of untreated ("*C"*) cells. (C) shows the effects of CK2α plus CK2α' knockdown on CSQ2 kinase activity levels measured in detergent extracts of treated (*si*) and untreated ("*C"*) COS cells. Plots show means ± S.E.M., n=3.

for subsequent experiments in cultured COS cells.

To determine the effect of CK2 knockdown on CSQ2 kinase activity, we transfected COS cells with siRNA directed at both isoforms of the catalytic subunit. Protein levels for both CK2 isoforms, determined by immunoblotting, were reduced by approximately 95% over controls (Fig. 23B). Extracts prepared from these siRNA-cells exhibited an approximate 2-fold reduction in CSQ2 kinase activity (Fig. 23C). This decrease in CSQ2 kinase activity is notable given the high levels of CK2 present in

COS cells (Fig. 20B) and the potential that siRNA does not silence all cellular pools of CK2 equally, such as those with differing rates of protein turnover. CSQ2 kinase activities from cells following silencing of individual CK2 isoforms could not resolve subunit-specific effects because of apparent compensatory changes in each CK2α

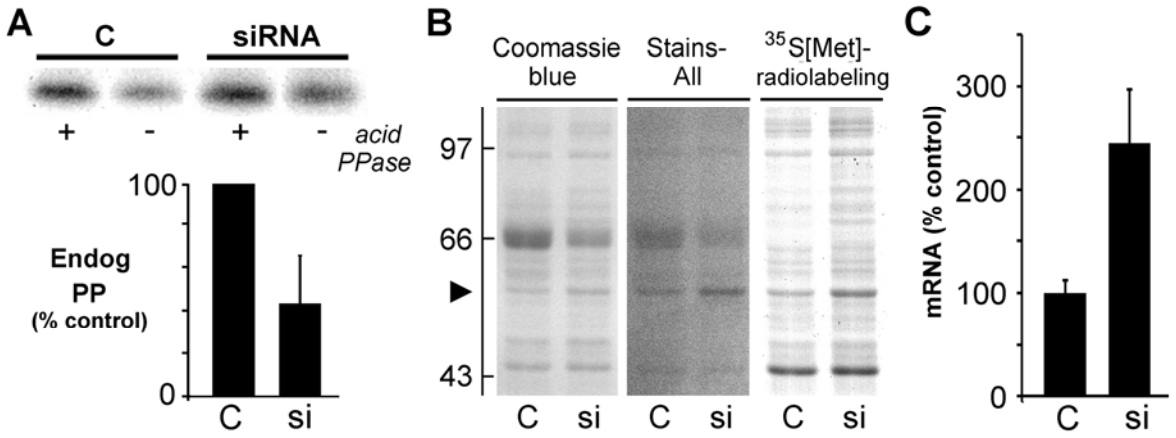

Figure 24. Reduction in endogenous CSQ2 phosphorylation in cells treated with CK2 siRNA. COS cells were treated with Ad.CSQ for 24 h in culture, then transfected with siRNA against CK2α plus CK2α' for an additional 48 h. (A) Cells were extracted in mild-detergent, and levels of phosphate on partially purified CSQ2 (Endog PP) were determined. Individual samples of CSQ2 were normalized by immunoblotting. A sample autoradiogram is shown for purified CSQ2 samples for untreated control ("C") and siRNA-treated COS cells (*upper panel*). Results are also shown (*lower panel*) from multiple analyses of endogenous CSQ2-phosphate content for C and siRNA-treated cells (means±S.E.M., n=4). (B) similar Ad.CSQ-treated COS cells (C or siRNA-treated) were metabolically labeled with ^{35}S[Met] for 2 h, and identical sample volumes were analyzed by SDS-PAGE. The gel was stained with Stains-All to highlight CSQ2 as a dark-blue protein band on a pink background (*arrowhead*), then destained and re-stained with Coomassie blue, then dried and placed against film for autoradiography. MW standards (*left*) are in kDa. The 66 kDa standard is albumin, which also contaminates the sample cultures from the serum in the medium. (C) effects of CK2 siRNA on CSQ2 mRNA levels determined by triplicate qPCR measurements (means ± S.E.M., n=3).

isoform that occurred after 48 h of knockdown.

To determine whether CK2 knockdown would decrease the level of endogenous CSQ2 phosphorylation in intact cells, COS cells overexpressing canine CSQ2 were treated with CK2 siRNA. In accordance with the roughly 2-fold decrease in CSQ2 kinase activity caused by CK2 siRNA transfection (Fig. 23C), we measured a 2-fold

decrease in the levels of phosphate in CSQ2 in COS cells (Fig. 24A). This loss of endogenous phosphate occurred despite a 24 h period of overexpression prior to siRNA treatment. Moreover, even with CK2 protein diminishing over the course of the treatment period, an ongoing phosphorylation of CSQ2 would have occurred due to the exquisite affinity of CSQ2 for CK2 [36].

A complicating effect of CK2 siRNA in COS cells was an increase in protein on SDS-gels, including significant changes in overexpressed CSQ2 (Fig. 24B). The change could be seen by protein stain, as well as following a 2 h [^{35}S]methionine labeling of cells. Analysis by qPCR of CSQ2 mRNA in treated and untreated cells showed a roughly 2-fold increase (Fig. 24C). Whether transcriptional or translational changes accounted for observed changes in cellular protein was not further investigated. Measurements of CSQ2 phosphorylation were therefore carried out by first purifying CSQ2 from cellular extracts, normalizing CSQ2 levels using antibody binding (immunoblot) analyses, then using standard phosphate analysis assays.

Effects of CSQ2 phosphorylation site mutation on protein trafficking in nonmuscle cells

To determine whether CSQ2 phosphorylation could affect its trafficking, we examined purified wild-type CSQ2 (CSQ-WT) and phosphorylation-site mutants (Table 2) by electrospray mass spectrometry to determine the details of their polymorphic structure [31]. CSQ-WT was composed primarily of molecules having glycans with

Table 2. CSQ2 phosphoform variants.

Name	cDNA	Phosphoform
CSQ-WT	-EDDDDDDGNNSDEESNDDSDDDD^{391}E-COOH	Phosphorylated on Ser 378, 382, 386
CSQ-nonPP	. . . . . A . . . A . . . A	Phosphorylation deficient
CSQ-mimPP	. . . . . E . . . E . . . E	Phosphomimetic

structures of GlcNAc2Man9 and GlcNAc2Man8 (Man9,8) with only minor amounts or no Man7 (Fig. 25A). In addition, these CSQ-WT molecules contained peaks of phosphorylated protein with a spacing of 81 Da (Fig. 25A, *shaded*) as previously described [23, 31]. Replacement of phosphorylatable serines with alanines (CSQ-nonPP) led to loss of all CSQ2 phosphorylation along with the appearance of lower-mass forms of the protein that correspond to increased levels of mannose trimming (Fig. 25B). We previously showed in COS cells that mannose trimming beyond Man9,8 occurs for CSQ2 molecules that are not efficiently retained in ER [23].

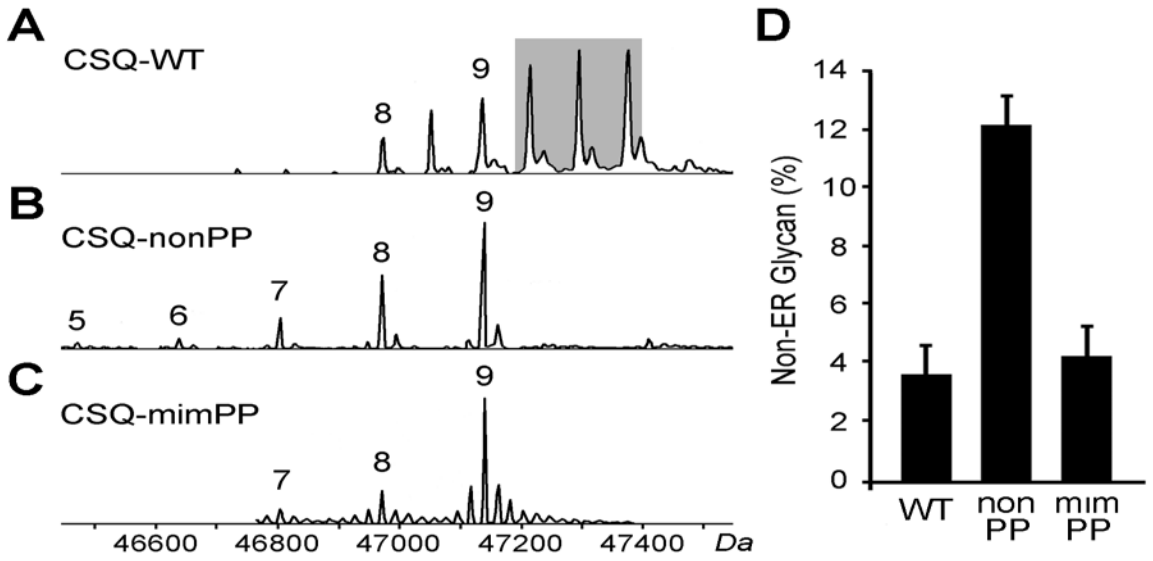

Figure 25. Effects of CSQ2 phosphorylation site sequence on glycan structure in nonmuscle cells. Cultured nonmuscle cells were treated with recombinant adenoviruses encoding either the wild-type CSQ2 sequence (*WT*), the Ser(378,382,386)Ala triple point mutant (*nonPP*), or the Ser(378,382,386)Glu mutant (*mimPP*) for 48 h, then CSQ2 was purified and analyzed by mass spectrometry as described in Experimental Procedures. Sample mass spectra are shown for each purified sequence of CSQ2 (A-C). Numbers 5-9 refer to the number of mannoses in the glycan that correspond to the mass values shown along the bottom axis. Minor levels of peaks that differ in mass by 20-40 Da, are likely to correspond to cation-bound molecules, and varied among spectra. Mannose content for the three CSQ2 structures are shown as aligned, although there were minor differences in mass due to the sequence mutations. Molecular weights (*bottom*) are those corresponding to the WT sequence. (D) The percentages of total CSQ2 molecules that exhibited mannosidase trimming to below 8 mannoses (non-ER glycan) are shown from multiple experiments (means ± S.E.M., n=3).

To determine whether this effect on CSQ2 trafficking was purely due to the loss of phosphorylatable serines, we carried out the same analysis following replacement of serines with glutamates (CSQ-mimPP). In contrast to CSQ-nonPP, CSQ-mimPP molecules gave structures similar to that of CSQ-WT (Fig. 25C). Multiple spectra from independent CSQ-WT, CSQ-nonPP and CSQ-mimPP samples were analyzed in order to compare the percent of total CSQ2 leaving ER as represented by mannoses less than 8 and 9 (Fig. 25D). Thus, the CSQ2 kinase appears to be acting at a co-translational site within the cell, and a resultant increase in CSQ2 phosphorylation may alter its ability to exit that site of biosynthesis.

DISCUSSION

CSQ2 kinase as protein kinase CK2

In mammalian heart tissue, CSQ2 exists as a highly phosphorylated protein [31, 34, 36]. Endogenous phosphate is found only on a cluster of 2 or 3 serine residues (depending upon the species) that are found in the cardiac C-terminal extension. This CSQ2 phosphorylation reaction is essentially the same in all mammalian cells examined to date, whether one examines native or overexpressed CSQ2 [23, 31]. In intact heart tissue, CSQ2 appears to be phosphorylated early in its biosynthesis in rough ER based upon the fact that newly synthesized molecules (Man 9,8,7) only exist in the fully phosphorylated state, whereas the most highly trimmed glycans (Man 2,3,4) are mostly devoid of phosphate [34]. A critical question that has remained unresolved in this process, however, is whether the CSQ2 kinase is protein kinase CK2. We previously showed that CSQ2 phosphorylation sites adhere closely to the consensus sequence for protein kinase CK2, and CSQ2 is exquisitely sensitive to CK2 *in vitro* [12]. However, if

CK2 is the CSQ2 kinase, it raises the important question of how CSQ2, a luminal ER protein, can be phosphorylated by what is believed to be a cytosolic enzyme. CK2 has no known mechanism for localizing to the ER/SR lumen where CSQ2 is thought to be wholly contained throughout its lifetime [17]. Only when the CSQ2 C-terminus is in the process of traversing the translocon pore complex could such an association theoretically occur [32]. Such a process suggests that CSQ2 phosphorylation is a co-translational event, and CK2 could be associated with the translocon, similar to the association of the oligosaccharide transferase complex (OST) that brings about co-translational N-linked glycosylation. CK2 has previously been shown to play a role in assembly of the translocon pore complex and signal sequence through phosphorylation of sec63 [112]. Calnexin, another resident ER protein, is a transmembrane protein that undergoes interaction with the ribosome in response to phosphorylation of its cytosolically exposed CK2 site [56]. We have previously reported that a number of resident ER/SR proteins are substrates for CK2 *in vitro* [17], perhaps suggesting that the reaction mechanism described in this paper may play a wider role in ER/SR biology.

To show that protein kinase CK2 is the physiological enzyme that modifies CSQ2 *in vivo*, this series of studies altered the reaction in a mammalian nonmuscle cell model system. Based upon our data from several experimental approaches, we conclude that CK2 is likely to be the native CSQ2 kinase that is present in all mammalian cells. This necessitates a co-translational or co-translocational phosphorylation event occurring for CSQ2. The differences we found in the glycan structures of CSQ2 phosphorylation site mutants support this conclusion, indicating that a proximal phosphorylation event affects subsequent CSQ2 trafficking, reflected in its mannose trimming, within the secretory

pathway.

CSQ2 kinase activity and its inhibition

Whether CK2 activity was competitively inhibited using TBCA, a highly specific inhibitor of CK2 [60], or biospecifically down-regulated using RNAi technology, CSQ2 kinase activity was affected in parallel. These data show that the CSQ2 kinase that exists in preparations derived from all mammalian cells [23] is likely the result of protein kinase CK2. Reduced levels of CSQ2 kinase that remain in cell extracts following CK2 inhibition or down-regulation, we believe, are unlikely to emanate from a second unknown CSQ2 kinase, although further studies may be warranted.

The advent of highly specific inhibitors of CK2 has also been driven by the fact that these compounds exhibit anti-growth and anti-cancer activities [58-59], reflecting an important role of CK2 in cell growth. The fact that CSQ2 is the major substrate for CK2 in heart homogenates is consistent with a possible role of CSQ2 phosphorylation in cardiac hypertrophy. We have previously shown that CSQ2 phosphorylation is doubled in canine tachycardia-induced heart failure [35].

In contrast to the relatively immediate inhibition of all available CK2 catalytic subunits using TBCA, siRNA inhibition was expected to be more gradual requiring turnover of the existing kinase pool, as suggested by Zhu et al. [59]. Furthermore, we cannot be certain that turnover of all CK2 pools within the cell are the same, whereas ATP binding sites are likely to be identical. Because both subunits are capable of efficiently phosphorylating CSQ2 *in vitro* (data not shown), simultaneous CK2α/α′ knockdown was needed to verify the identity of CK2 as CSQ2 kinase. Analysis by immunoblot usually showed a putative compensatory increase in subunit partner in

single subunit down-regulation experiments that was not further investigated. In spite of these differences in mechanisms, both CK2 inhibition techniques produced qualitative decreases in CSQ2 kinase activity, and each was able to lower phosphate incorporation in overexpressed CSQ2. Minor quantitative differences in the degrees of CSQ2 kinase inhibition were likely to have reflected their very different mechanisms of CK2 inhibition.

Experimental determinations of CSQ2 kinase and phosphorylation

Measurements of *in vitro* CSQ2 phosphorylation were found to be surprisingly nonlinear; and in fact produced lower levels of CSQ2 phosphorylation using higher levels of protein in the phosphorylation assay. In principle, the problems we uncovered should plague any and all determinations of kinase activity in crude preparations, such as those used in this study. Our data suggest that endogenous ATPases represent potentially confounding activities, such that it is necessary to use minimal cellular protein extract along with mild extraction techniques to accurately determine *in vitro* phosphorylation rates. Understanding these limitations, we were able to demonstrate the potential utility of these CK2 inhibitors for use as cellular probes.

Studies aimed at determining effects of CK2 reduction on phosphate levels in CSQ2 were carried out in CSQ2-adenovirus treated cells. As previously observed from ^{32}P-labeling reactions in cultured rat cardiomyocytes [34], the higher rate of CSQ2 biosynthesis obtained through Ad.CSQ2 treatment was needed to observe phosphorylation, presumably because of its elevated rate of biosynthesis and co-translational phosphorylation. CK2 silencing itself, however, produced increases in cellular and CSQ2 protein synthesis that affected steady state protein levels after 48 h in culture, as well as [^{35}S]Met incorporation over a 2 h period (Fig. 24B). CSQ2

purification, however, permitted measurements of CSQ2 phosphorylation state by using our standard assay with equal amounts of CSQ2. Thus, reductions of CK2 activity through either of two separate approaches in cultured cells reduced levels of cellular CSQ2 kinase activity, and reduced endogenous CSQ2 phosphate content.

Protein kinase CK2 regulation of CSQ2 trafficking

Based upon identification of CSQ2 kinase in intact cells as the cytosolic protein kinase CK2, our previous hypothesis that CSQ2 phosphorylation is a co-translational

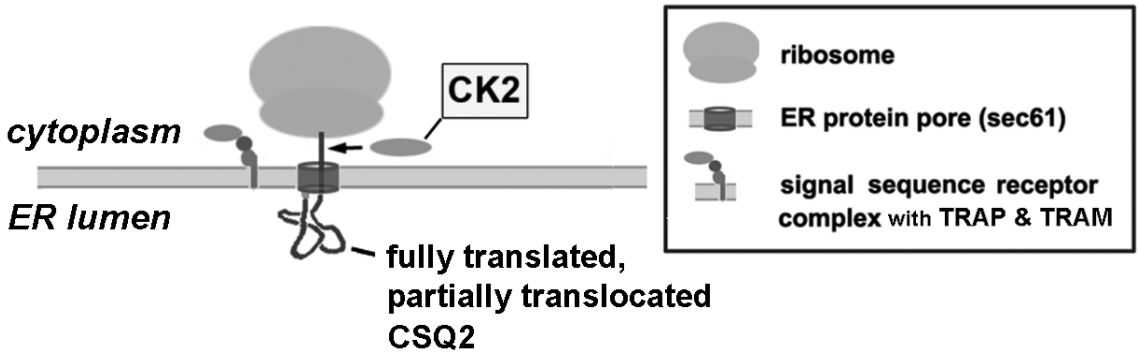

Figure 26. Hypothetical mechanism of cardiac CSQ phosphorylation by CK2 in rough ER during translocation across the ER membrane. A mechanism whereby an ER protein such as CSQ2 becomes exposed to cytoplasmic CK2 would require that the ER-bound ribosome permits access to the nascent CSQ2 polypeptide after completion of translation but during its translocation through the translocon. Other known translocon accessory proteins, such as TRAP and TRAM [99] are present in cardiomyocyte rough ER and could function in such translocational regulation [64].

event [34] can be expanded. In our new model (Fig. 26), we hypothesize that CSQ2 phosphorylation occurs before the C-terminal tail has entered the lumen of the protein pore complex (sec61) or ER lumen [113]. One possible mechanism might be a translocation pause wherein the ribosome separates from the translocon permitting a transient co-localization of CK2 and CSQ2 [64, 113]. If such a process, so proximal in the secretory pathway, were to affect the subsequent trafficking of CSQ2 through the secretory pathway, mannose trimming alterations would not be unexpected.

Intracellular localization of CSQ2 can consistently be predicted from its N-linked glycan structure in a number of mammalian cell types including cardiomyocytes. In this study, comparisons of glycan structures for CSQ-WT, CSQ-nonPP, and CSQ-mimPP showed that only the CSQ-nonPP form exhibits excessive mannose trimming, indicative of increased trafficking away from rough ER. Glutamate, a commonly used phosphomimetic substitution, showed a marked reversal of this effect on glycan structure. These results support the idea that CSQ2 phosphorylation is associated with its biosynthesis and affects retention of CSQ2 in ER.

In heart failure, the detailed structure of CSQ2 is dramatically shifted. A peak of newly synthesized CSQ2 (with Man9,8 glycans) accumulates instead of continuing through its normal trafficking cycle [35], indicating that this newly synthesized protein is being retained within rough ER structures. Rough ER, as we have recently demonstrated, is localized to juxtanuclear cisternae in cardiomyocytes [99]. Together with findings reported here, we hypothesize that changes in CK2 activity and/or localization in heart failure increase CSQ2 phosphorylation with consequent ER retention, to favor a perinuclear Ca^{2+} microdomain shift facilitating increased transcription or translation in hypertrophy.

CONCLUSIONS

In conclusion, findings generated from multiple experimental approaches in this study support an emerging picture of CSQ2 phosphorylation as a co-translational process, which we now hypothesize is co-translocational as well. Verification that CK2 is the *in vivo* CSQ2 kinase implicates the involvement of the rough ER translocon in this biological reaction. The dependence of CSQ2 glycan structure on its state of

phosphorylation has consistently revealed important features of this reaction, both here using CSQ2 phosphorylation site mutants as well as for CSQ2 in failing hearts. These studies should guide future investigations by establishing a basic biochemical paradigm for CSQ2 phosphorylation in the mammalian cell.

CHAPTER 4

SUMMARY

Cardiac CSQ is a multifaceted protein, capable of binding significant quantities of Ca^{2+} and altering RyR2 activity at junctional SR. The site of CSQ2 synthesis, however, is not junctional SR. This fact has been largely overlooked in the field of cardiac cell biology, coinciding with a tendency to picture protein distribution in the cardiomyocyte as a static system. The reality is that CSQ2 is constantly being made and trafficked from its site of biosynthesis in perinuclear rough ER to junctional SR in a polymer/monomer, phosphorylation-dependent manner.

With the majority of cardiac biochemists focusing on junctional SR Ca^{2+} release, little thought has been given to the basic questions that one assumes would have been answered prior to the study of complex cell biology. Accordingly, the location of rough ER in cardiomyocytes has never been elucidated. There is often a comparison between skeletal muscle myocytes, for which cell biology is slightly more established, and cardiac myocytes. This extrapolation may not be applicable in terms of protein synthesis however as traditional cell biology dictates that rough ER surrounds the nucleus and would therefore increase if more nuclei were present. This is the case as skeletal muscle cells are polynucleated while cardiac muscle cells are binucleated in a symmetrical manner.

Through the use of multiple antibodies specific to classic rough ER markers, and with the CSQ-DsRed fusion protein, we were able to establish a juxtanuclear localization of rough ER in cardiomyocytes. Using fluorescence confocal microscopy, the translocon complex proteins TRAP-α and TRAM, along with the ribosomal protein

S6, were all visualized and found to encapsulate both myonuclei. Additionally, time course studies of the CSQ-DsRed tetramer, in conjunction with anti-DsRed immunostaining, highlighted a perinuclear rough ER site of biosynthesis for CSQ2 and presumably all other proteins in the secretory system.

Following CSQ-DsRed translation, the fusion protein built up in the ER surrounding the nuclei due to DsRed tetramerization, and then trafficked anterogradely to junctional SR. Filling of more peripheral junctional SR puncta occurred with increasing incubation time. With the exception of CSQ-DsRed concentration around the nuclei, DsRed fusion protein tetramerization-dependent trafficking is predicted to be very similar to CSQ2 polymerization-dependent trafficking likely caused by the Ca^{2+} properties of secretory pathway compartments.

Cardiac-specific C-terminal phosphorylation of CSQ2 serines was also shown to effect CSQ2 trafficking according to mass spectrometric analysis of the protein's N-linked glycan. A Ser 378,382,386 Ala mutation (CSQ-nonPP) of these sites inhibited CSQ2 phosphorylation and led to an increased trafficking out of the ER as indicated by the increased mannose trimming of CSQ2 glycan. This effect was reversed with the phosphomimetic mutant Ser 378,382,386 Glu (CSQ-mimPP) which had glycoforms with mannose trimming nearly identical to that of CSQ-WT.

Pharmacological and molecular inhibition were used to establish the identity of CSQ2 kinase as protein kinase CK2. *In vitro*, inhibition of CSQ2 phosphorylation using cardiomyocyte and nonmuscle cell CSQ2 kinase sources was successfully carried out with three specific inhibitors of CK2: TBB, DMAT and TBCA. TBCA produced identical inhibition curves for both cellular kinase sources and commercial CK2α′ kinase, with

increasing concentrations of drug. SiRNA knockdown of both CK2α and CK2α′ catalytic subunits in nonmuscle cells reduced CSQ2 kinase activity by nearly 2-fold according to similar *in vitro* CSQ2 phosphorylation assays.

Additionally, both ATP-binding site competitive inhibition and CK2 RNAi protein inhibition were used successfully *in situ* to suppress endogenous CSQ2 phosphorylation. TBCA used at 100 μM with CSQ-WT overexpressing cardiomyocytes and COS nonmuscle cells in culture led to an 82 and 66% decrease in CSQ2 phosphate incorporation, respectively, compared to control. Similarly, simultaneous knockdown of both CK2α and CK2α′ catalytic subunits in COS cells overexpressing adenoviral CSQ-WT, caused a near 2-fold decrease in CSQ2 phosphate incorporation, further supporting the identity of CSQ2 kinase as protein kinase CK2.

These studies present a global model for CSQ2 trafficking regulation in cardiomyocytes. As CSQ2 is translated at perinuclear rough ER, its C-terminus is exposed to the cytosolic protein kinase CK2 allowing for CSQ2 phosphorylation prior to translocation into the ER lumen. A combination of dephosphorylation and monomerization then promote anterograde trafficking through the secretory system. CSQ2 subsequently becomes retained in junctional SR compartments due to increasing Ca^{2+} concentrations, which leads to polymer formation. Following a decrease in Ca^{2+} levels, CSQ2 monomerizes to once again traffic anterogradely through the secretory system.

APPENDIX

LIST OF ABBREVIATIONS

Ad.CSQ	wild-type cardiac calsequestrin adenovirus
Ad.CSQ-DsRed	adenoviral cardiac calsequestrin-DsRed
Ad.CSQ-HA	adenoviral cardiac calsequestrin with hemagglutinin epitope tag
Ad.mimPP	constitutively-phosphorylated cardiac calsequestrin adenovirus
Ad.nonPP	nonphosphorylatable cardiac calsequestrin adenovirus
CICR	calcium-induced calcium release
COS	COS-7 African green monkey kidney cells
CPVT	catecholaminergic polymorphic ventricular tachycardia
CSNK2A1	protein kinase CK2α catalytic subunit
CSNK2A2	protein kinase CK2α′ catalytic subunit
CSQ	calsequestrin
CSQ-DsRed	cardiac calsequestrin pDsRed2-N1 fusion protein
CSQ-mimPP	constitutively-phosphorylated cardiac calsequestrin
CSQ-nonPP	nonphosphorylatable cardiac calsequestrin
CSQ-WT	wild-type cardiac calsequestrin
CSQ1	skeletal calsequestrin
CSQ2	cardiac calsequestrin
CSQ-HA	cardiac calsequestrin with hemagglutinin epitope tag
DAPI	4′-6-diamidino-2-phenylindole
DMAT	2-dimethylamino-4,5,6,7-tetrabromo-1H-benzimidazole
DMEM	Dulbecco’s Modified Eagle’s Medium

DRB	5,6-dichloro-1-(β-D-ribofuranosyl)-benzimidazole
DsiRNA	Dicer-Substrate siRNA
ECL	electrochemiluminescence
ER	endoplasmic reticulum
ERGIC	ER-Golgi intermediate compartment
ESMS	electrospray mass spectrometry
GlcNAc	N-acetyl-D-glucosamine
HEK	human embryonic kidney 293 cells
HF	heart failure
HRP	horseradish peroxidase
IP3R	inositol trisphosphate receptor
Jct	junctin
Man	mannose
MOI	multiplicity of infection
NCX	Na^+/Ca^{2+} exchanger
OST	oligosacharyl transferase complex
RNC	ribosome nascent chain complex
RyR	ryanodine receptor
RyR2	cardiac ryanodine receptor
SERCA2a	cardiac sarco/endoplasmic reticulum Ca^{2+}-ATPase
SP/SPC	signal peptidase complex
SR	sarcoplasmic reticulum
SRP	signal recognition particle

SRP-R	signal recognition particle receptor
T-tubules	transverse tubules
TBCA	tetrabromocinnamic acid
TBB	4,5,6,7-tetrabromobenzotriazole
TRAM	translocating chain-associated membrane protein
TRAP	translocon-associated protein complex
Trd/Trd1	triadin-1

REFERENCES

1. Mohrman DE, Heller LJ. Cardiovascular physiology. 6th ed: The McGraw-Hill Companies; 2006.
2. Chung MK, Rich MW. (1990). Introduction to the cardiovascular system. *Alcohol Health and Research World, 14*(4), 269-76.
3. MayoClinic.com. Heart muscle. [cited 2010; Available from: http://www.ohiohealth.com/mayo/images/image_popup/r7_heartmuscle.jpg
4. University_of_Cambridge_Department_of_Pathology. Normal myocardium. 2009 [cited 2010; Available from: http://www.path.cam.ac.uk/Normal/CR_Cardiorespiratory/HT_Heart/N_CR_HT_03.jpg
5. Gottlieb RA, Burleson KO, Kloner RA, Babior BM, Engler RL. (1994). Reperfusion injury induces apoptosis in rabbit cardiomyocytes. *J Clin Invest, 94*(4), 1621-8.
6. Sommer JR. (1995). Comparative anatomy: in praise of a powerful approach to elucidate mechanisms translating cardiac excitation into purposeful contraction. *J Mol Cell Cardiol, 27*(1), 19-35.
7. Boron WF, Boulpaep EL. Medical physiology: a cellular and molecular approach. Updated ed: Elsevier; 2005.
8. Berridge MJ, Bootman MD, Roderick HL. (2003). Calcium signalling: dynamics, homeostasis and remodelling. *Nat Rev Mol Cell Biol, 4*(7), 517-29.

9. Gyorke I, Hester N, Jones LR, Gyorke S. (2004). The role of calsequestrin, triadin, and junctin in conferring cardiac ryanodine receptor responsiveness to luminal calcium. *Biophys J, 86*(4), 2121-8.

10. Jorgensen AO, Kalnins VI, Zubrzycka E, MacLennan DH. (1977). Assembly of the sarcoplasmic reticulum. Localization by immunofluorescence of sarcoplasmic reticulum proteins in differentiating rat skeletal muscle cell cultures. *J Cell Biol, 74*(1), 287-98.

11. Campbell KP, MacLennan DH, Jorgensen AO, Mintzer MC. (1983). Purification and characterization of calsequestrin from canine cardiac sarcoplasmic reticulum and identification of the 53,000 dalton glycoprotein. *J Biol Chem, 258*(2), 1197-204.

12. Cala SE, Jones LR. (1983). Rapid purification of calsequestrin from cardiac and skeletal muscle sarcoplasmic reticulum vesicles by Ca2+-dependent elution from phenyl-sepharose. *J Biol Chem, 258*(19), 11932-6.

13. Terentyev D, Viatchenko-Karpinski S, Gyorke I, Volpe P, Williams SC, Gyorke S. (2003). Calsequestrin determines the functional size and stability of cardiac intracellular calcium stores: Mechanism for hereditary arrhythmia. *Proc Natl Acad Sci U S A, 100*(20), 11759-64.

14. Jorgensen AO, Shen AC, Campbell KP, MacLennan DH. (1983). Ultrastructural localization of calsequestrin in rat skeletal muscle by immunoferritin labeling of ultrathin frozen sections. *J Cell Biol, 97*(5 Pt 1), 1573-81.

15. Jorgensen AO, Campbell KP. (1984). Evidence for the presence of calsequestrin in two structurally different regions of myocardial sarcoplasmic reticulum. *J Cell Biol, 98*(4), 1597-602.

16. Franzini-Armstrong C, Kenney LJ, Varriano-Marston E. (1987). The structure of calsequestrin in triads of vertebrate skeletal muscle: a deep-etch study. *J Cell Biol, 105*(1), 49-56.

17. Cala SE, Scott BT, Jones LR. (1990). Intralumenal sarcoplasmic reticulum Ca(2+)-binding proteins. *Semin Cell Biol, 1*(4), 265-75.

18. Bers DM. Calcium sources and sinks. Excitation and Contraction Coupling and Cardiac Contractile Force. 2nd ed. Dordrecht/Boston/London: Kluwer Academic Publishers; 2001, p. 39-56.

19. MacLennan DH, Wong PT. (1971). Isolation of a calcium-sequestering protein from sarcoplasmic reticulum. *Proc Natl Acad Sci U S A, 68*(6), 1231-5.

20. Ikemoto N, Bhatnager GM, Gergely J. (1971). Fractionation of solubilized sarcoplasmic reticulum. *Biochem Biophys Res Commun, 44*(6), 1510-7.

21. Fliegel L, Burns K, Wlasichuk K, Michalak M. (1989). Peripheral membrane proteins of sarcoplasmic and endoplasmic reticulum. Comparison of carboxyl-terminal amino acid sequences. *Biochem Cell Biol, 67*(10), 696-702.

22. Jorgensen AO, McLeod AG, Campbell KP, Denney GH. (1984). Evidence for the presence of calsequestrin in both peripheral and interior regions of sheep Purkinje fibers. *Circ Res, 55*(2), 267-70.

23. Houle TD, Ram ML, McMurray WJ, Cala SE. (2006). Different endoplasmic reticulum trafficking and processing pathways for calsequestrin (CSQ) and epitope-tagged CSQ. *Exp Cell Res, 312*(20), 4150-61.

24. Wang S, Trumble WR, Liao H, Wesson CR, Dunker AK, Kang CH. (1998). Crystal structure of calsequestrin from rabbit skeletal muscle sarcoplasmic reticulum. *Nature structural biology, 5*(6), 476-83.

25. Park H, Park IY, Kim E, Youn B, Fields K, Dunker AK, et al. (2004). Comparing skeletal and cardiac calsequestrin structures and their calcium binding: a proposed mechanism for coupled calcium binding and protein polymerization. *J Biol Chem, 279*(17), 18026-33.

26. Park H, Wu S, Dunker AK, Kang C. (2003). Polymerization of calsequestrin. Implications for Ca2+ regulation. *J Biol Chem, 278*(18), 16176-82.

27. Jones LR, Suzuki YJ, Wang W, Kobayashi YM, Ramesh V, Franzini-Armstrong C, et al. (1998). Regulation of Ca2+ signaling in transgenic mouse cardiac myocytes overexpressing calsequestrin. *J Clin Invest, 101*(7), 1385-93.

28. Knollmann BC, Chopra N, Hlaing T, Akin B, Yang T, Ettensohn K, et al. (2006). Casq2 deletion causes sarcoplasmic reticulum volume increase, premature Ca2+ release, and catecholaminergic polymorphic ventricular tachycardia. *J Clin Invest, 116*(9), 2510-20.

29. Song L, Alcalai R, Arad M, Wolf CM, Toka O, Conner DA, et al. (2007). Calsequestrin 2 (CASQ2) mutations increase expression of calreticulin and ryanodine receptors, causing catecholaminergic polymorphic ventricular tachycardia. *J Clin Invest, 117*(7), 1814-23.

30. Knollmann BC. (2009). New roles of calsequestrin and triadin in cardiac muscle. *J Physiol, 587*(Pt 13), 3081-7.

31. O'Brian JJ, Ram ML, Kiarash A, Cala SE. (2002). Mass spectrometry of cardiac calsequestrin characterizes microheterogeneity unique to heart and indicative of complex intracellular transit. *J Biol Chem, 277*(40), 37154-60.

32. Helenius A, Aebi M. (2001). Intracellular functions of N-linked glycans. *Science, 291*(5512), 2364-9.

33. Scott BT, Simmerman HK, Collins JH, Nadal-Ginard B, Jones LR. (1988). Complete amino acid sequence of canine cardiac calsequestrin deduced by cDNA cloning. *J Biol Chem, 263*(18), 8958-64.

34. Ram ML, Kiarash A, Marsh JD, Cala SE. (2004). Phosphorylation and dephosphorylation of calsequestrin on CK2-sensitive sites in heart. *Mol Cell Biochem, 266*(1-2), 209-17.

35. Kiarash A, Kelly CE, Phinney BS, Valdivia HH, Abrams J, Cala SE. (2004). Defective glycosylation of calsequestrin in heart failure. *Cardiovasc Res, 63*(2), 264-72.

36. Cala SE, Jones LR. (1991). Phosphorylation of cardiac and skeletal muscle calsequestrin isoforms by casein kinase II. Demonstration of a cluster of unique rapidly phosphorylated sites in cardiac calsequestrin. *J Biol Chem, 266*(1), 391-8.

37. Kuenzel EA, Mulligan JA, Sommercorn J, Krebs EG. (1987). Substrate specificity determinants for casein kinase II as deduced from studies with synthetic peptides. *J Biol Chem, 262*(19), 9136-40.

38. Marin O, Meggio F, Marchiori F, Borin G, Pinna LA. (1986). Site specificity of casein kinase-2 (TS) from rat liver cytosol. A study with model peptide substrates. *Eur J Biochem, 160*(2), 239-44.

39. Allende JE, Allende CC. (1995). Protein kinases. 4. Protein kinase CK2: an enzyme with multiple substrates and a puzzling regulation. *Faseb J, 9*(5), 313-23.

40. Johnson SA, Hunter T. (2005). Kinomics: methods for deciphering the kinome. *Nature methods, 2*(1), 17-25.

41. Gyenis L, Litchfield DW. (2008). The emerging CK2 interactome: insights into the regulation and functions of CK2. *Mol Cell Biochem, 316*(1-2), 5-14.

42. Cala SE, Miles K. (1992). Phosphorylation of the cardiac isoform of calsequestrin in cultured rat myotubes and rat skeletal muscle. *Biochim Biophys Acta, 1118*(3), 277-87.

43. Ahmed K, Gerber DA, Cochet C. (2002). Joining the cell survival squad: an emerging role for protein kinase CK2. *Trends in cell biology, 12*(5), 226-30.

44. Litchfield DW. (2003). Protein kinase CK2: structure, regulation and role in cellular decisions of life and death. *The Biochemical journal, 369*(Pt 1), 1-15.

45. Litchfield DW, Luscher B. (1993). Casein kinase II in signal transduction and cell cycle regulation. *Mol Cell Biochem, 127-128*, 187-99.

46. Guerra B, Boldyreff B, Sarno S, Cesaro L, Issinger OG, Pinna LA. (1999). CK2: a protein kinase in need of control. *Pharmacology & therapeutics, 82*(2-3), 303-13.

47. Channavajhala P, Seldin DC. (2002). Functional interaction of protein kinase CK2 and c-Myc in lymphomagenesis. *Oncogene, 21*(34), 5280-8.

48. Kelliher MA, Seldin DC, Leder P. (1996). Tal-1 induces T cell acute lymphoblastic leukemia accelerated by casein kinase IIalpha. *Embo J, 15*(19), 5160-6.

49. Landesman-Bollag E, Channavajhala PL, Cardiff RD, Seldin DC. (1998). p53 deficiency and misexpression of protein kinase CK2alpha collaborate in the development of thymic lymphomas in mice. *Oncogene, 16*(23), 2965-74.

50. French AC, Luscher B, Litchfield DW. (2007). Development of a stabilized form of the regulatory CK2beta subunit that inhibits cell proliferation. *J Biol Chem, 282*(40), 29667-77.

51. Litchfield DW, Bosc DG, Canton DA, Saulnier RB, Vilk G, Zhang C. (2001). Functional specialization of CK2 isoforms and characterization of isoform-specific binding partners. *Mol Cell Biochem, 227*(1-2), 21-9.

52. Xu X, Toselli PA, Russell LD, Seldin DC. (1999). Globozoospermia in mice lacking the casein kinase II alpha' catalytic subunit. *Nature genetics, 23*(1), 118-21.

53. Zhang C, Vilk G, Canton DA, Litchfield DW. (2002). Phosphorylation regulates the stability of the regulatory CK2beta subunit. *Oncogene, 21*(23), 3754-64.

54. Pinna LA. (2002). Protein kinase CK2: a challenge to canons. *Journal of cell science, 115*(Pt 20), 3873-8.

55. Kubinski K, Domanska K, Sajnaga E, Mazur E, Zielinski R, Szyszka R. (2007). Yeast holoenzyme of protein kinase CK2 requires both beta and beta' regulatory subunits for its activity. *Mol Cell Biochem, 295*(1-2), 229-36.

56. Chevet E, Wong HN, Gerber D, Cochet C, Fazel A, Cameron PH, et al. (1999). Phosphorylation by CK2 and MAPK enhances calnexin association with ribosomes. *EMBO J, 18*(13), 3655-66.

57. Faust M, Jung M, Gunther J, Zimmermann R, Montenarh M. (2001). Localization of individual subunits of protein kinase CK2 to the endoplasmic reticulum and to the Golgi apparatus. *Mol Cell Biochem, 227*(1-2), 73-80.

58. Kaminska B, Ellert-Miklaszewska A, Oberbek A, Wisniewski P, Kaza B, Makowska M, et al. (2009). Efficacy and mechanism of anti-tumor action of new potential CK2 inhibitors toward glioblastoma cells. *Int J Oncol, 35*(5), 1091-100.

59. Zhu D, Hensel J, Hilgraf R, Abbasian M, Pornillos O, Deyanat-Yazdi G, et al. (2010). Inhibition of protein kinase CK2 expression and activity blocks tumor cell growth. *Mol Cell Biochem, 333*(1-2), 159-67.

60. Pagano MA, Poletto G, Di Maira G, Cozza G, Ruzzene M, Sarno S, et al. (2007). Tetrabromocinnamic acid (TBCA) and related compounds represent a new class of specific protein kinase CK2 inhibitors. *Chembiochem, 8*(1), 129-39.

61. Sarno S, Pinna LA. (2008). Protein kinase CK2 as a druggable target. *Molecular bioSystems, 4*(9), 889-94.

62. Mishra S, Pertz V, Zhang B, Kaur P, Shimada H, Groffen J, et al. (2007). Treatment of P190 Bcr/Abl lymphoblastic leukemia cells with inhibitors of the serine/threonine kinase CK2. *Leukemia, 21*(1), 178-80.

63. Duncan JS, Gyenis L, Lenehan J, Bretner M, Graves LM, Haystead TA, et al. (2008). An unbiased evaluation of CK2 inhibitors by chemoproteomics:

characterization of inhibitor effects on CK2 and identification of novel inhibitor targets. *Mol Cell Proteomics, 7*(6), 1077-88.

64. Hegde RS, Kang SW. (2008). The concept of translocational regulation. *J Cell Biol, 182*(2), 225-32.

65. Johnson AE, van Waes MA. (1999). The translocon: a dynamic gateway at the ER membrane. *Annu Rev Cell Dev Biol, 15*, 799-842.

66. Kalies KU, Hartmann E. (1998). Protein translocation into the endoplasmic reticulum (ER)--two similar routes with different modes. *Eur J Biochem, 254*(1), 1-5.

67. Jorgensen AO, Shen AC, Campbell KP. (1985). Ultrastructural localization of calsequestrin in adult rat atrial and ventricular muscle cells. *J Cell Biol, 101*(1), 257-68.

68. Gyorke S, Terentyev D. (2008). Modulation of ryanodine receptor by luminal calcium and accessory proteins in health and cardiac disease. *Cardiovasc Res, 77*(2), 245-55.

69. Royer L, Rios E. (2009). Deconstructing calsequestrin. Complex buffering in the calcium store of skeletal muscle. *J Physiol, 587*(Pt 13), 3101-11.

70. Franzini-Armstrong C. (2009). Architecture and regulation of the Ca2+ delivery system in muscle cells. *Appl Physiol Nutr Metab, 34*(3), 323-7.

71. Milstein ML, Houle TD, Cala SE. (2009). Calsequestrin isoforms localize to different ER subcompartments: evidence for polymer and heteropolymer-dependent localization. *Exp Cell Res, 315*(3), 523-34.

72. Cho JH, Ko KM, Singaruvelu G, Lee W, Kang GB, Rho SH, et al. (2007). Functional importance of polymerization and localization of calsequestrin in C. elegans. *Journal of cell science, 120*(Pt 9), 1551-8.

73. Dunphy WG, Brands R, Rothman JE. (1985). Attachment of terminal N-acetylglucosamine to asparagine-linked oligosaccharides occurs in central cisternae of the Golgi stack. *Cell, 40*(2), 463-72.

74. Laemmli UK. (1970). Cleavage of structural proteins during the assembly of the head of bacteriophage T4. *Nature, 227*(5259), 680-5.

75. Lowry HO, Rosebrough NJ, Farr AL, Randall RJ. (1951). Protein measurements with folin phenol reagent. *J Biol Chem, 193*, 265-75.

76. Wall MA, Socolich M, Ranganathan R. (2000). The structural basis for red fluorescence in the tetrameric GFP homolog DsRed. *Nature structural biology, 7*(12), 1133-8.

77. Campbell RE, Tour O, Palmer AE, Steinbach PA, Baird GS, Zacharias DA, et al. (2002). A monomeric red fluorescent protein. *Proc Natl Acad Sci U S A, 99*(12), 7877-82.

78. Fons RD, Bogert BA, Hegde RS. (2003). Substrate-specific function of the translocon-associated protein complex during translocation across the ER membrane. *J Cell Biol, 160*(4), 529-39.

79. Hartmann E, Gorlich D, Kostka S, Otto A, Kraft R, Knespel S, et al. (1993). A tetrameric complex of membrane proteins in the endoplasmic reticulum. *Eur J Biochem, 214*(2), 375-81.

80. Gorlich D, Hartmann E, Prehn S, Rapoport TA. (1992). A protein of the endoplasmic reticulum involved early in polypeptide translocation. *Nature, 357*(6373), 47-52.

81. Barlowe C. (2000). Traffic COPs of the early secretory pathway. *Traffic, 1*(5), 371-7.

82. Barlowe C, Orci L, Yeung T, Hosobuchi M, Hamamoto S, Salama N, et al. (1994). COPII: a membrane coat formed by Sec proteins that drive vesicle budding from the endoplasmic reticulum. *Cell, 77*(6), 895-907.

83. Tang BL, Ong YS, Huang B, Wei S, Wong ET, Qi R, et al. (2001). A membrane protein enriched in endoplasmic reticulum exit sites interacts with COPII. *J Biol Chem, 276*(43), 40008-17.

84. Orci L, Ravazzola M, Meda P, Holcomb C, Moore HP, Hicke L, et al. (1991). Mammalian Sec23p homologue is restricted to the endoplasmic reticulum transitional cytoplasm. *Proc Natl Acad Sci U S A, 88*(19), 8611-5.

85. Houle TD, Ram ML, Cala SE. (2004). Calsequestrin mutant D307H exhibits depressed binding to its protein targets and a depressed response to calcium. *Cardiovasc Res, 64*(2), 227-33.

86. Rivera VM, Wang X, Wardwell S, Courage NL, Volchuk A, Keenan T, et al. (2000). Regulation of protein secretion through controlled aggregation in the endoplasmic reticulum. *Science, 287*(5454), 826-30.

87. Slade AM, Severs NJ. (1985). Rough endoplasmic reticulum in the adult mammalian cardiac muscle cell. *J Submicrosc Cytol, 17*(4), 531-6.

88. Antony C, Huchet M, Changeux JP, Cartaud J. (1995). Developmental regulation of membrane traffic organization during synaptogenesis in mouse diaphragm muscle. *J Cell Biol, 130*(4), 959-68.

89. Kaisto T, Metsikko K. (2003). Distribution of the endoplasmic reticulum and its relationship with the sarcoplasmic reticulum in skeletal myofibers. *Exp Cell Res, 289*(1), 47-57.

90. Volpe P, Villa A, Podini P, Martini A, Nori A, Panzeri MC, et al. (1992). The endoplasmic reticulum-sarcoplasmic reticulum connection: distribution of endoplasmic reticulum markers in the sarcoplasmic reticulum of skeletal muscle fibers. *Proc Natl Acad Sci U S A, 89*(13), 6142-6.

91. Cala SE, Jones LR. (1994). GRP94 resides within cardiac sarcoplasmic reticulum vesicles and is phosphorylated by casein kinase II. *J Biol Chem, 269*(8), 5926-31.

92. Cala SE. (1999). Determination of a putative phosphate-containing peptide in calreticulin. *Biochem Biophys Res Commun, 259*(2), 233-8.

93. Pelham HR. (1995). Sorting and retrieval between the endoplasmic reticulum and Golgi apparatus. *Curr Opin Cell Biol, 7*(4), 530-5.

94. Rahkila P, Alakangas A, Vaananen K, Metsikko K. (1996). Transport pathway, maturation, and targetting of the vesicular stomatitis virus glycoprotein in skeletal muscle fibers. *Journal of cell science, 109 (Pt 6)*, 1585-96.

95. Higazi DR, Fearnley CJ, Drawnel FM, Talasila A, Corps EM, Ritter O, et al. (2009). Endothelin-1-stimulated InsP3-induced Ca2+ release is a nexus for hypertrophic signaling in cardiac myocytes. *Mol Cell, 33*(4), 472-82.

96. Jones LR, Cala SE. (1981). Biochemical evidence for functional heterogeneity of cardiac sarcoplasmic reticulum vesicles. *J Biol Chem, 256*(22), 11809-18.

97. Fliegel L, Ohnishi M, Carpenter MR, Khanna VK, Reithmeier RA, MacLennan DH. (1987). Amino acid sequence of rabbit fast-twitch skeletal muscle calsequestrin deduced from cDNA and peptide sequencing. *Proc Natl Acad Sci U S A, 84*(5), 1167-71.

98. Yano K, Zarain-Herzberg A. (1994). Sarcoplasmic reticulum calsequestrins: structural and functional properties. *Mol Cell Biochem, 135*(1), 61-70.

99. McFarland TP, Milstein ML, Cala SE. (2010). Rough endoplasmic reticulum to junctional sarcoplasmic reticulum trafficking of calsequestrin in adult cardiomyocytes. *J Mol Cell Cardiol, 49*(4), 556-64.

100. Lozeman FJ, Litchfield DW, Piening C, Takio K, Walsh KA, Krebs EG. (1990). Isolation and characterization of human cDNA clones encoding the alpha and the alpha' subunits of casein kinase II. *Biochemistry, 29*(36), 8436-47.

101. Olsten ME, Litchfield DW. (2004). Order or chaos? An evaluation of the regulation of protein kinase CK2. *Biochem Cell Biol, 82*(6), 681-93.

102. Wirkner U, Voss H, Lichter P, Ansorge W, Pyerin W. (1994). The human gene (CSNK2A1) coding for the casein kinase II subunit alpha is located on chromosome 20 and contains tandemly arranged Alu repeats. *Genomics, 19*(2), 257-65.

103. Yang-Feng TL, Naiman T, Kopatz I, Eli D, Dafni N, Canaani D. (1994). Assignment of the human casein kinase II alpha' subunit gene (CSNK2A1) to chromosome 16p13.2-p13.3. *Genomics, 19*(1), 173.

104. Alvarado-Diaz CP, Tapia JC, Antonelli M, Moreno RD. (2009). Differential localization of alpha' and beta subunits of protein kinase CK2 during rat spermatogenesis. *Cell Tissue Res, 338*(1), 139-49.

105. Yu IJ, Spector DL, Bae YS, Marshak DR. (1991). Immunocytochemical localization of casein kinase II during interphase and mitosis. *J Cell Biol, 114*(6), 1217-32.

106. Guerra B, Issinger OG. (1999). Protein kinase CK2 and its role in cellular proliferation, development and pathology. *Electrophoresis, 20*(2), 391-408.

107. Tawfic S, Yu S, Wang H, Faust R, Davis A, Ahmed K. (2001). Protein kinase CK2 signal in neoplasia. *Histol Histopathol, 16*(2), 573-82.

108. Lowry OH, Rosebrough NJ, Farr AL, Randall RJ. (1951). Protein measurement with the Folin phenol reagent. *J Biol Chem, 193*(1), 265-75.

109. Sanger F, Nicklen S, Coulson AR. (1977). DNA sequencing with chain-terminating inhibitors. *Proc Natl Acad Sci U S A, 74*(12), 5463-7.

110. Ruzzene M, Penzo D, Pinna LA. (2002). Protein kinase CK2 inhibitor 4,5,6,7-tetrabromobenzotriazole (TBB) induces apoptosis and caspase-dependent degradation of haematopoietic lineage cell-specific protein 1 (HS1) in Jurkat cells. *The Biochemical journal, 364*(Pt 1), 41-7.

111. Schneider CC, Hessenauer A, Gotz C, Montenarh M. (2009). DMAT, an inhibitor of protein kinase CK2 induces reactive oxygen species and DNA double strand breaks. *Oncol Rep, 21*(6), 1593-7.

112. Wang X, Johnsson N. (2005). Protein kinase CK2 phosphorylates Sec63p to stimulate the assembly of the endoplasmic reticulum protein translocation apparatus. *Journal of cell science, 118*(Pt 4), 723-32.

113. Hegde RS, Lingappa VR. (1999). Regulation of protein biogenesis at the endoplasmic reticulum membrane. *Trends in cell biology, 9*(4), 132-7.

ABSTRACT

CARDIAC CALSEQUESTRIN PHOSPHORYLATION AND TRAFFICKING IN THE MAMMALIAN CARDIOMYOCYTE

by

TIMOTHY P. MCFARLAND

May 2011

Advisor: Dr. Steven E. Cala

Major: Physiology

Degree: Doctor of Philosophy

Cardiac CSQ (CSQ2) is a multifaceted protein, capable of binding significant quantities of Ca^{2+} and altering ryanodine receptor activity at the junctional sarcoplasmic reticulum (SR). Little is known about the trafficking of CSQ2 from its unknown site of biosynthesis, which appears to be of importance as its structure changes in a trafficking-dependent manner in various types of heart failure. Through the use of multiple antibodies specific to classic rough ER markers, and with the creation of CSQ-DsRed tetramer fusion protein, we were able to establish a juxtanuclear localization of rough ER in cardiomyocytes. Using fluorescence confocal microscopy, the translocon complex proteins TRAP-α and TRAM, along with the ribosomal protein S6, were all visualized and found to encapsulate both myonuclei. Additionally, time course studies of CSQ-DsRed, in conjunction with anti-DsRed immunostaining, highlighted a perinuclear rough ER site of biosynthesis for CSQ2. The fusion protein exhibited a tetramerization-dependent trafficking predicted to be very similar to CSQ2 polymerization-dependent trafficking with high and low secretory compartment Ca^{2+} concentrations leading to polymerization and monomerization, respectively.

Cardiac-specific C-terminal phosphorylation of CSQ2 serines was shown to effect CSQ2 trafficking according to mass spectrometric analysis of the protein's N-linked glycan. A Ser 378,382,386 Ala mutation (CSQ-nonPP) of these sites inhibited CSQ2 phosphorylation and led to an increased trafficking out of the ER as indicated by the increased mannose trimming of CSQ2 glycan. This effect was reversed with the phosphomimetic mutant Ser 378,382,386 Glu (CSQ-mimPP) which had glycoforms with mannose trimming nearly identical to that of CSQ-WT.

Pharmacological and molecular inhibition were used to establish the identity of CSQ2 kinase as protein kinase CK2. *In vitro*, inhibition of CSQ2 phosphorylation using cardiomyocyte and nonmuscle cell CSQ2 kinase sources was successfully carried out with three specific inhibitors of CK2: TBB, DMAT and TBCA. TBCA produced identical inhibition curves for both cellular kinase sources and commercial CK2α′ kinase, with increasing concentrations of drug. SiRNA knockdown of both CK2α and CK2α′ catalytic subunits in nonmuscle cells reduced CSQ2 kinase activity by nearly 2-fold according to similar *in vitro* CSQ2 phosphorylation assays.

Additionally, both ATP-binding site competitive inhibition and CK2 RNAi protein inhibition were used successfully *in situ* to suppress endogenous CSQ2 phosphorylation. TBCA used at 100 μM with CSQ-WT overexpressing cardiomyocytes and COS nonmuscle cells in culture led to an 82 and 66% decrease in CSQ2 phosphate incorporation, respectively, compared to control. Similarly, simultaneous knockdown of both CK2α and CK2α′ catalytic subunits in COS cells overexpressing adenoviral CSQ-WT, caused a near 2-fold decrease in CSQ2 phosphate incorporation, further supporting the identity of CSQ2 kinase as protein kinase CK2.

These studies present a global model for CSQ2 trafficking regulation in cardiomyocytes. As CSQ2 is translated at perinuclear rough ER, its C-terminus is exposed to the cytosolic protein kinase CK2 allowing for CSQ2 phosphorylation prior to translocation into the ER lumen. A combination of dephosphorylation and monomerization then promotes anterograde trafficking through the secretory system. CSQ2 subsequently becomes retained in junctional SR compartments due to increasing Ca^{2+} concentrations, which led to polymer formation. Following a decrease in Ca^{2+} levels, CSQ2 monomerizes to once again traffic anterogradely through the secretory system.

AUTOBIOGRAPHICAL STATEMENT

Name: Timothy P. McFarland

Education: Bachelor of Science, 2004
Michigan State University
Major: Biochemistry and Molecular Biology/Biotechnology
East Lansing, MI

I have always enjoyed the prospect of making a career out of solving problems. Initially, I was an electrical engineering major at Michigan State University where I learned to appreciate physics and mathematics. I had never thought of entering into science, but soon after my first general chemistry course, I discovered my passion for the field and transferred into the Biochemistry and Molecular Biology department. Fortunately, I was able to keep the fact that I was a science nerd under wraps, allowing me to meet my future wife Lindsay a few years prior to graduation. Upon completing my B.S. degree in 2004, I began work as a pharmacy technician for the hematology/oncology/nephrology unit of the Children's Hospital of Michigan. This clinical experience led me to pursue my Ph.D. through the Department of Physiology, where I worked for five years under the expert supervision of Dr. Steven E. Cala. This is where I developed my love for cardiovascular biochemistry and cell biology. I hope to stay in this field in order to establish an academic career.